IEEE Access
Multidisciplinary : Rapid Review : Open Access Journal

Received 3 December 2023, accepted 17 December 2023, date of publication 25 December 2023,
date of current version 16 January 2024.

Digital Object Identifier 10.1109/ACCESS.2023.3346533

RESEARCH ARTICLE

Optimal Allocation of TCSC Devices in Transmission Power Systems by a Novel Adaptive Dwarf Mongoose Optimization

HASHIM ALNAMI[1], ALI M. EL-RIFAIE[2], (Senior Member, IEEE), GHAREEB MOUSTAFA[1], SULTAN H. HAKMI[1], ABDULLAH M. SHAHEEN[3], AND MOHAMED A. TOLBA[4,5], (Senior Member, IEEE)

[1]Electrical Engineering Department, College of Engineering, Jazan University, Jazan 45142, Saudi Arabia
[2]College of Engineering and Technology, American University of the Middle East, Egaila 54200, Kuwait
[3]Department of Electrical Engineering, Faculty of Engineering, Suez University, Suez, Egypt
[4]Nuclear Research Center, Reactors Department, Egyptian Atomic Energy Authority, Cairo 11787, Egypt
[5]Electrical Power Systems Department, National Research University "MPEI," 111250 Moscow, Russia

Corresponding authors: Ali M. El-Rifaie (ali.el-rifaie@aum.edu.kw) and Abdullah M. Shaheen (abdullah.mohamed.eng19@suezuni.edu.eg)

ABSTRACT This paper introduces a novel Improved Dwarf Mongoose Optimizer (IDMO) based on an Alpha-Directed Learning Process (ADLP) for dealing with different mathematical benchmark models and engineering problems. The dwarf mongoose's foraging behavior motivated the DMO's primary design. Three social groupings are used: the alpha group, babysitters, and scouts. The unique suggested solution includes an upgraded ADLP to boost searching abilities, and its upgrading mechanism is substantially led by the improved alpha. First, the IDMO and DMO are put through their paces using CEC 2017 single objective optimization benchmarks. Also, several recent optimization techniques are taken into contrast, including artificial ecosystem optimization (AEO), aquila optimization (AQU), equilibrium optimization (EO), enhanced slime mould algorithm (ESMA), Gorilla troops optimization (GTO), red kite optimization (RKO), subtraction-average-based algorithm (SAA) and slime mould algorithm (SMA). Further, their application validity is examined for optimal allocation of Thyristor Controlled Series Capacitor (TCSC) devices in transmission power systems. The simulations are implemented on two different IEEE power systems of 30 and 57 buses, and considering different numbers of TCSC devices. The suggested IDMO and DMO are compared to several different current and popular techniques for all applications. The findings from the simulation demonstrate that, in relation to efficiency and effectiveness, the suggested DMO beats not only the standard DMO but also a large number of other contemporary solutions. For the first system, considering three TCSC devices to be optimized and based on the mean acquired losses, the proposed IDMO accomplishes 5.65%, 0.68%, 3.72%, 16.44%, and 5.88% reduction in power losses in compared to DMO, SAA, AEO, Grey Wolf Optimizer (GWO) and AQU, respectively. Similarly, for the second system, the proposed IDMO achieves improvement reduction 28.96%, 54.20%, 9.44%, 60.99% and 48.54%, respectively, compared to the obtained results by the DMO, SAA, AEO, GWO and AQU.

INDEX TERMS Dwarf Mongoose optimizer, alpha-directed learning process, thyristor controlled series capacitor technology, power systems, power losses minimization.

NOMENCLATURE OF ACRONYMS

ACPTDF	AC Power Transfer Distribution Factor.
ADLP	Alpha-Directed Learning Process.
AEO	Artificial Ecosystem Optimizer.
AGC	Automatic Generation Control.
AQU	Aquila Algorithm.
ATC	Available Transfer Capability.

The associate editor coordinating the review of this manuscript and approving it for publication was Ali Raza.

BBO	Biogeography Based Optimization.
CSSO	Chaotic Salp Swarm Optimizer.
DE	Differential Evolution.
DMO	Dwarf Mongoose Optimizer.
ECSA	Emended Crow Search Algorithm.
EM	Electromagnetism-like Mechanism.
EO	Equilibrium Optimization.
ESMA	Enhanced Slime Mould Algorithm.
FACTS	Flexible Alternating Current Transmission Systems.
GA	Genetic Algorithm.
GBOA	Gradient-Based Optimization Algorithm.
GWO	Grey Wolf Optimizer.
GTO	Gorilla Troops Optimizer.
HP	Helogale Parvula.
IPSO	Improved Particle Swarm Optimization.
IDMO	Improved Dwarf Mongoose Optimization.
ITSE	Integral of Time multi-plied Squared Error.
IWO	Invasive Weed Optimization.
OPFI	Optimal Power Flow Issue.
PID	Proportional Integral Derivative.
PPS	Powell's Pattern Search.
PSO	Particle Swarm Optimization.
QMFT	Quantum computing with Moth Flame Technique.
RKO	Red Kite Optimization.
SAA	Subtraction-Average-based Algorithm.
SMA	Slime Mould Algorithm.
SSSC	Static synchronous series compensator.
TCSC	Thyristor Controlled Series Capacitor.
TCPS	Thyristor controlled phase shifter.
TLBO	Teaching-Learning Based Optimization.
WCEMFT	Water Cycle Emerged with Moth Flame Technique.
WOA	Whale Optimization Algorithm.

I. INTRODUCTION

A. MOTIVATION

The electrical network that makes up the power system is a complex one, very large in size, and it consists of loads, distribution and transmission systems, and generating stations. These networks are dispersed across a very large geographic area. In recent years, consumption of electricity has been increasing at an exponential rate, necessitating constant efforts by the power network sectors in the generation, transmission, and distribution of electrical power [1]. These sectors continue to promote their strategies in order to preserve the framework for competition in the electricity market. The primary goal is to develop deregulation of electricity production throughout the world in an attempt to create competitive marketplaces for buying and selling electric power. The deregulated energy market presents a slew of innovative technological hurdles to electrical market participants [2], [3], [4]. All-generation firms and distribution companies compete for the most profitable transactions in a restructured environment [5].

In practical electrical networks, TCSC technology is frequently used as a powerful and cost-effective series FACTS device with high performance, enabling precise and secure OPFI management of power lines [6]. The series-compensating characteristics provided by TCSC make it one of the most cost-effective methods of releasing the transmission network's capacity to transport additional real power [7], [8]. In order to minimize tie-line power and area frequency fluctuations, three series of FACTS devices of TCSC, TCPS and SSSC were considered and simulated in AGC investigations regarding multi-area connected electrical systems [9]. The damping controllers in this work have been developed using an IPSO technique and the ITSE minimization objective. The suggested TCSC-AGC performed better than TCPS and SSSC in terms of damping of vibrations, tie-line transmitted powers, and area frequencies. In addition, tests of sensitivity have been carried out to demonstrate the TCSC-AGC's resilience. This concluding finding demonstrated the importance and beneficial advantages of the TCSC over the SSSC in transmission systems, and therefore it reveals its applicability in real life.

B. LITERATURE REVIEW

In order to address OPFI, academic scholars have lately developed a variety of classical and metaheuristic optimization approaches [10]. Newton-based methods [13], linear and nonlinear programming, gradient approaches, interior point methods [12], sequential unconstrained methodology [11], and fuzzy linear methods [11] are some of the conventional approaches. Nevertheless, it should be highlighted that such approaches are ineffective for huge electrical networks and do not create perfect solutions. As a result, scholars have sought to establish metaheuristic approaches to overcome the shortcomings of older methodologies. Numerous of these methods have high convergence properties and can effectively impose inequality boundaries. However, these traditional approaches may become stuck at a local minimum since they rely on the initial configuration and are unable to produce the true optimal result. Additionally, each approach needs to be modelled with specific OPFI variants, and they are unable to handle discrete and integer variables with ease. Therefore, it is crucial to create metaheuristic methods to get around the aforementioned drawbacks. In the recent two decades, there has been a tendency towards employing various heuristic (population-based) strategies to address a variety of OPFI difficulties [12] [13]. To deal with the OPFI, several population-based algorithms such as the EM approach [14], SAA [15], TLBO [16], GA [17], GWO and DE [18], CSSO [19], GBOA [20], BBO [21], PSO [22], WCEMFT [23], and QMFT [24] are utilized. In addition, in [25], the TLBO approach was created and used to solve the allocation optimization problem of capacitor devices in electrical systems for the purpose of power factor adjustment.

Diverse augmentations of the techniques' strategies have been characterized to reduce the energy loss of the OPFI. The equation for solutions that depend on the best and worst solutions for losses and voltage profile has been adjusted for JAYA in [26]. In ref [27], an enhanced social spider optimizer was described to reduce power losses by balancing the movement patterns of male and female spiders. In [28], the IWO has been emerged with PPS including a combinational strategy for OPFI investigation with the addition of FACTS. GTO was used on the OPFI with IEEE 30 bus system in [29]. The GTO incorporates five methods for gorilla collective actions: engaging other gorillas, moving to an unknown location, travelling in a specific orientation, competing for adult females, and pursuing the silverback. GTO was used on the OPFI with the addition of the TCSC modules in [30]. Nevertheless, the size and allocation of the TCSC were not considered. An ECSA was used on the OPFI, as shown in [31], including modifications to combine an innovative bat strategy. In [32], a placement methodology based on combined sensitivity indices was presented to install TCSC in power systems considering the situations of normal operation and line outages. In this study, the performance index and the ranking index were combined where the performance index selects the severe lines based on contingency cases while the ranking index selects the severe lines based on the system loading level for a specific outage. Despite the work in [32] derived significant mitigation the line overloads on transmission lines in the event of a network outage in IEEE 5 bus and 14 bus networks, it missed the determination of the suitable sizing of the TCSC in the investigated networks which has strong impacts on such applications. In [33], an improved version of GA was introduced to determine the optimal location and compensation level of TCSC devices. The presented GA was incorporated with dual mutation probability in order to enhance the available transfer capability in power systems. In [34], a modified version of SAA is presented for the allocation of TCSC for reducing losses in electrical power grids. This study incorporates a cooperative learning technique based on the leader solution into the standard SAA. In [35], a multi-objective particle swarm optimization has been carried out for multi-objective optimal allocation model for TCSC in order to improve the available transfer capability and the voltage stability utilizing the L index. In this study, a chaos initialization technique was introduced, and a variable inertia weight setting was implemented which is applied for only one transmission grid of the IEEE-30 bus system.

Dwarf Mongoose Optimizer (DMO) is a revolutionary approach created by studying the foraging behavior of Helogale Parvula (HP) animals (dwarf mongoose's) [36]. It uses the alpha category, babysitters, and scouts as distinct HP social groupings. The entire group seeks together, with the alpha female beginning off and choosing the path, geographical distance, and sleeping locations [37]. Because of its outstanding broadly searching capacity and adaptability, it has been employed in tackling a variety of real-world engineering optimization problems [38], [39], [40], [41], [42], [43], [44], [45]. Table 1 describes several recent variants of the DMO that are developed and designed for solving different engineering problems.

C. MAIN OBJECTIVE OF THIS WORK

The main objective of this work is dedicated for optimal allocation of TCSC devices in transmission power systems. In this regard, an innovative Improved Dwarf Mongoose Optimizer (IDMO) is presented. To prove its effectiveness, it is tested for CEC 2017 benchmarks. Also, it is developed to solve the TCSC allocation problem considering two different IEEE power systems of 30 and 57 buses and considering different number of TCSC devices. The suggested IDMO and DMO are compared to a number of different current and popular techniques for all applications. The findings from the simulation demonstrate that, in relation to efficiency and effectiveness, the suggested DMO beats not only the standard DMO but also a large number of other contemporary solutions.

D. PAPER CONTRIBUTIONS

This study suggests an innovative Improved Dwarf Mongoose Optimizer (IDMO) incorporating the Alpha-Directed Learning Process (ADLP) for addressing various mathematical benchmark functions and engineering difficulties. The unique suggested solution includes an improved ADLP to boost searching capacities, and its upgrading procedure is substantially led by the amended alpha. Firstly, the proposed IDMO and DMO are put through their paces using CEC 2017 benchmarks. Further, the proposed IDMO is adopted for optimal allocation of TCSC devices in transmission power systems in order to minimize the overall system losses. Additionally, the proposed IDMO's accuracy and superiority of solution are demonstrated in comparison to the others while considering various numbers of TCSC devices.

The main contributions cited in this study include the following:

- The study introduces a distinctive IDMO technique, including ADLP, which has been proven to have a significant advantage over conventional DMO in several CEC 2017 benchmark works. The TCSC devices' positioning and size have been strategically managed to minimize power losses, unlike previous efforts.
- The suggested IDMO outperforms the DMO and other contemporary methods like AEO, SAA, and AQU in handling this situation.

II. ALLOCATION OF TCSC DEVICES IN TRANSMISSION POWER SYSTEMS: PROBLEM FORMULATION

A. MODELLING OF TCSC DEVICES

The TCSC has become one of the significantly commonly used FACTS components belonging to the series type, which offers a lot of advantages such as high performance, quick

TABLE 1. Several variants of DMO for solving different engineering problems.

Ref.	DMO Version	Validation on benchmarks	Applications
[38]	Standard form	-	Frequency control for Power System with solar energy and Storage Device
[39]	Standard form	-	Prediction of Thermal Expansion of Nanocomposites
[41]	A novel DMO variation including a quantum-based optimization is showcased. The sampling of the set for testing is first split into training and testing. The next step is to determine the starting value for a group of people who reflect the answer to the problem being evaluated. Then, employing the sample of training, calculate each person's fitness value and assign the best value to them. The present solutions are then updated by using the DMO operators.	-	Feature Selection problem
[44]	Combining the DMO with the mutualism phase of Symbiotic Organism Search results in a hybrid technique.	-	Generation Expansion Planning in electrical systems
[45]	A new approach that applies intelligent optimization algorithms utilizing three main parts of DMO, generalized normal distribution, and opposition-based learning strategy.	Twenty-three benchmark functions	Data clustering applications
[46]	Based on improving the Prairie Dog optimization algorithm's searching procedure by utilizing the DMO's main update mechanism, a hybrid algorithm is presented.	Twenty-three benchmark functions	-
[47]	A new controlling operator that regulates the alpha motion is used to change the alpha choice in a modified DMO that is provided. Also, randomization is used to alter the motions of the scout group. Furthermore, the criteria for switching babysitters have been adjusted such that, upon meeting the requirement, the swapping babysitters communicate with the DMOs in order to share information.	CEC 2020 benchmark functions	Engineering Design Problems such as welded beam, compression and pressure vessel design problems
[48]	A hybrid approach is presented by combining the AEO with DMO.	eighteen CEC2017, and ten CEC2019 benchmark functions	Feature selection problem

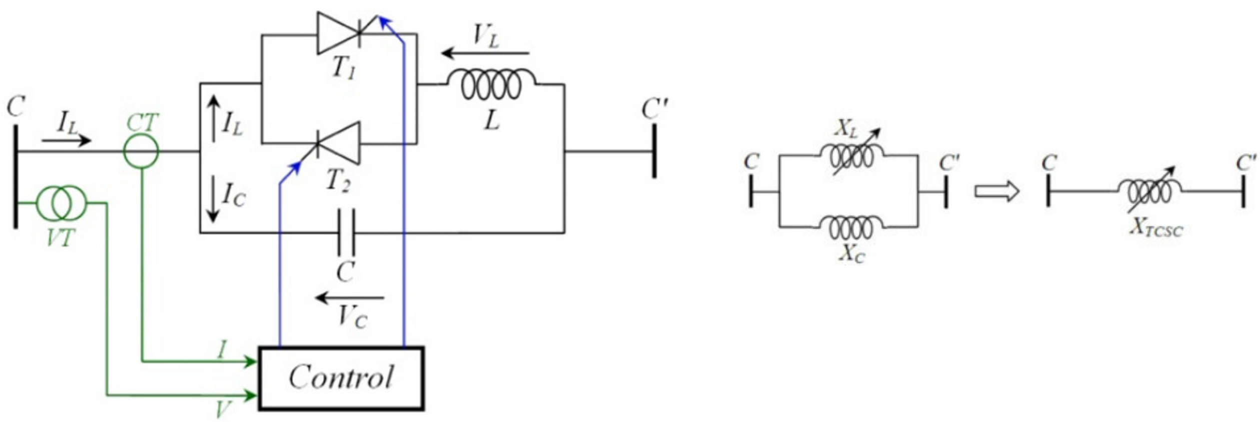

(a) Mounting (b) Apparent Reactance

FIGURE 1. Transmission line with installed TCSC.

reaction, and low cost. The two reactive modes of operation that are accessible to TCSC systems include inductive and capacitive. As a result, the reactance of the relevant transmission line is able to be adjusted in increasing or decreasing directions. Figure 1(a) depicts the TCSC model in power networks linked in series with a line. It is made up of a capacitance (C) linked in parallel with an inductance (L), that is regulated by a valve situated in two thyristors (T1 and T2). The angle of extinction (α), which may be set to any value between 90° and 180°, determines how the valve operates [49].

A variable capacitive reactance (X_{TCSC}) was injected into the transmission line by the compensator TCSC as depicted in Fig. 1(b). The regulated thyristors' angle (α), which can range from 90° to 180° and is defined by the subsequent equation, directly affects how X_{TCSC} is represented [50], [51]. As a consequence, the transmission-line reactance (X_{Line}) is used to symbolize the TCSC's reactance. To prevent transmission line overcompensation, the TCSC device's (X_{TCSC}) required value can be calculated using Eq. (1) [52], [53]:

$$X_{TCSC}(\alpha) = \frac{X_L(\alpha) \times X_C}{X_L(\alpha) + X_C} \tag{1}$$

$$X_L(\alpha) = \left(\frac{\pi}{\pi - sin(2\alpha) - 2\alpha}\right) X_{L\,,max} \tag{2}$$

$$X_{L\,,max} = (2\pi f)\, L,\ \ X_C = \frac{-1}{j\,(2\pi f)\, C} \tag{3}$$

substituting the terms $X_L(\alpha)$ and X_C, Eq. (1) will be formulated as follows:

$$X_{TCSC}(\alpha) = \frac{\left(\frac{\pi}{\pi - sin(2\alpha) - 2\alpha}\right) X_{L\,,max} \times X_C}{\left(\frac{\pi}{\pi - sin(2\alpha) - 2\alpha}\right) X_{L\,,max} + X_C} \tag{4}$$

B. TCSC ALLOCATION-BASED LOSSES MINIMIZATION AND CONSTRAINTS

To technically improve the electrical system and the overall voltage profile, the main objective is to minimise overall network losses, which could be computationally portrayed as follows [54]:

$$OJ = \sum_{m=1}^{Nbus} \left(\sum_{\substack{n=1 \\ m \neq n}}^{Nbus} G_{mn}(V_m^2 + V_n^2 - 2 \times (V_m V_n cos\,(\theta_{mn})) \right) \tag{5}$$

where N_{bus} represents the number of buses; G_{mn} reflects the conductance of the transmission line connected between buses m and n; θ_{mn} and V_{mn} displayed the difference regarding phase angle and voltage, respectively between the buses m and n.

To handle the TCSC allocation issue; many inequalities and equality constraints relating to both dependent and independent variables have to be fulfilled.

The control variables regarding the optimal TCSC allocation problems are:

1. Reactance compensation of each TCSC device to be installed.
2. Candidate transmission lines to be selected for each TCSC device to be installed.
3. Reactive power injection from existing Var sources in the transmission system.
4. Generator voltage
5. Generator output powers
6. Tap settings of the transformers.

The requirements for independent variables, reactance compensation, and TCSC locations must be met, as indicated in Eqs. (6) and (7), accordingly.

$$-50\% X_{Line_{TCSC,k}} \geq X_{TCSC}(\alpha)_k \geq +50\% X_{Line_{TCSC,p}},\quad k = 1, 2, \ldots N_{TCSC} \tag{6}$$

$$N_{lines} \geq Line_{TCSC,k} \geq 1, k = 1, 2, \ldots N_{TCSC} \tag{7}$$

where $Line_{TCSC,k}$ denote the potential lines for installing TCSC systems; N_{lines} denotes the total number of transmission lines; N_{TCSC} indicates the number of TCSC equipment that will be placed; $X_{Line_{TCSC,k}}$ indicates the reactance of the respective lines which have been selected for installing TCSC equipment.

In terms of independent variables, Eqs. (8)-(11) manage the constraints for reactive power injection from Var sources, generator voltage, generator output powers, and tap settings, accordingly.

$$QI_{Vr}^{min} \leq QI_{Vr} \leq QI_{Vr}^{max},\ Vr = 1, 2, \ldots Nq \tag{8}$$

$$Vg_m^{min} \leq Vg_m \leq Vg_m^{max},\ m = 1, 2, \ldots Ng \tag{9}$$

$$Pg_m^{min} \leq Pg_m \leq Pg_m^{max},\ m = 1, 2, \ldots Ng \tag{10}$$

$$Tp_k^{min} \leq Tp_k \leq Tp_k^{max},\ k = 1, 2, ..Nt \tag{11}$$

where Nq denotes the total number of VAr sources, Ng signifies the total number of generating units, and Nt denotes the total number of transformers. Pg depicts the actual power output of generators; Tp stands for the tap values regarding tap transformers. The voltages of the generators are represented by Vg, whereas the injected reactive power of VAr sources is represented by QI.

In addition, in terms of variables that are dependent, Eqs. (12)-(14) are used to address the constraints for buses voltage, apparent power flow over the transmission lines, and reactive powers output of the generators.

$$V_m^{min} \leq V_m \leq V_m^{max},\ m = 1, 2, \ldots .Nbus \tag{12}$$

$$|SF_L| \leq SFl_L^{max},\ L = 1, 2, \ldots .N_{lines} \tag{13}$$

$$Qg_m^{min} \leq Qg_m \leq Qg_m^{max},\ m = 1, 2, \ldots Ng \tag{14}$$

where Qg specifies the produced reactive power from generators and SF denotes transmission flow limitations.

The active and reactive power loading balance calculations at every bus, on the other hand, must be kept as equality restrictions. These limitations are entirely met using the load flow routine's completion.

III. IDMO FOR SOLVING THE OPTIMAL TCSC ALLOCATION

A. DMO

Dwarf Mongoose Optimizer (DMO) is developed by the foraging behavior of the Helogale Parvula (HP) animals (dwarf mongoose's) [36]. The HP animals' population in the DMO is divided into three distinct hierarchical groups: the alpha category, scouts, and babysitters. The alpha is the leader of the entire group. Babysitters are provided by a subgroup of the HP animals group, and they are often a mix of both gender kinds. They will remain beside the youngsters till the remainder of the gathering comes later in the afternoon. The babysitters are initially switched for the purpose to continue feeding with the others. The HP animal family does not

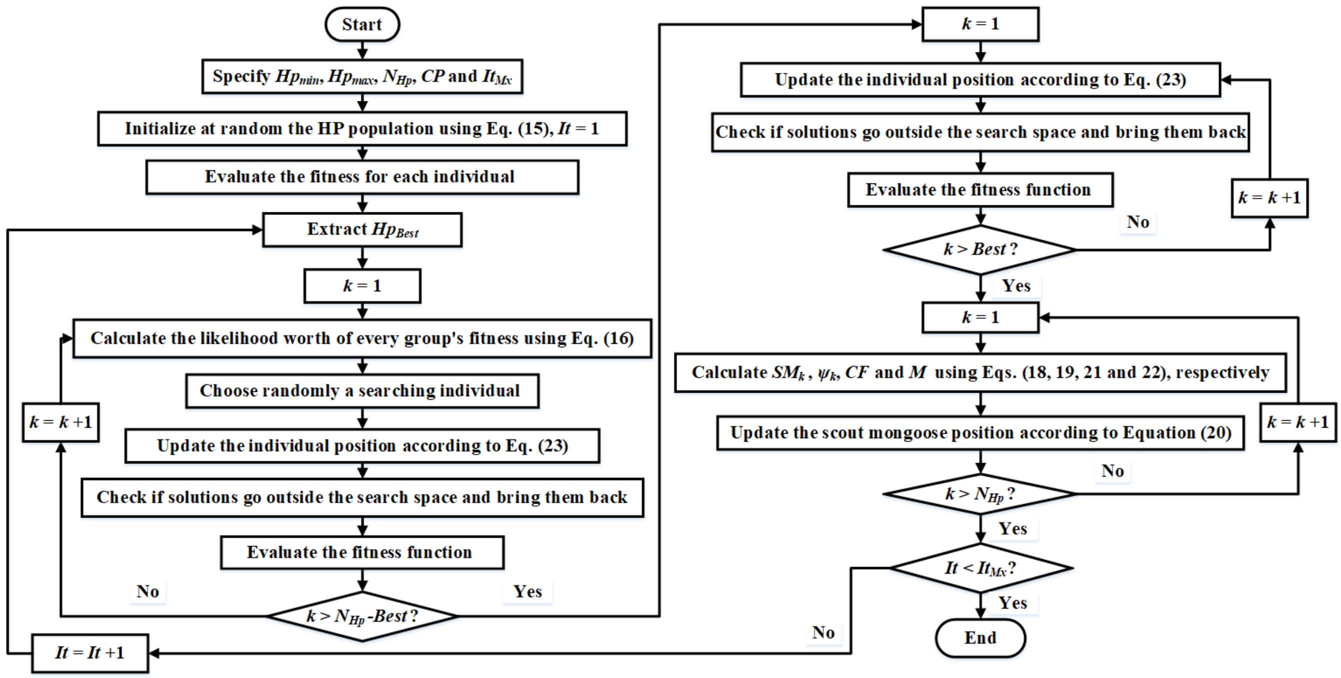

FIGURE 2. Proposed IDMO flowchart.

TABLE 2. Mathematical data of the benchmarks regarding CEC 2017.

No.	Function	Optimal	No.	Function	Optimal
Fn_1	Shifted and Rotated Bent Cigar	100	Fn_2	Shifted and Rotated Zakharov	300
Fn_3	Shifted and Rotated Rosenbrock's	400	Fn_4	Shifted and Rotated Rastrigin's	500
Fn_5	Shifted and Rotated Expanded Scaffer's F6	600	Fn_6	Shifted and Rotated Lunacek Bi_Rastrigin	700
Fn_7	Shifted and Rotated Non-Continuous Rastrigin's	800	Fn_8	Shifted and Rotated Levy	900
Fn_9	Shifted and Rotated Schwefel's	1000	Fn_{10}	Hybrid 1 (N = 3)	1100
Fn_{11}	Hybrid 2 (N = 3)	1200	Fn_{12}	Hybrid 3 (N = 3)	1300
Fn_{13}	Hybrid 4 (N = 4)	1400	Fn_{14}	Hybrid 5 (N = 4)	1500
Fn_{15}	Hybrid 6 (N = 4)	1600	Fn_{16}	Hybrid 6 (N = 5)	1700
Fn_{17}	Hybrid 6 (N = 5)	1800	Fn_{18}	Hybrid 6 (N = 5)	1900
Fn_{19}	Hybrid 6 (N = 6)	2000	Fn_{20}	Composition 1 (N = 3)	2100
Fn_{21}	Composition 2 (N = 3)	2200	Fn_{22}	Composition 3 (N = 4)	2300
Fn_{23}	Composition 4 (N = 4)	2400	Fn_{24}	Composition 5 (N = 5)	2500
Fn_{25}	Composition 6 (N = 5)	2600	Fn_{26}	Composition 7 (N = 6)	2700
Fn_{27}	Composition 8 (N = 6)	2800	Fn_{28}	Composition 9 (N = 3)	2900

construct a nest to shelter their young; alternatively, they constantly shift their resting mound in search of a fresh area. The HP animals have formed a semi-nomadic way of life. It ensures that every square area is examined, thus guaranteeing no formerly journeyed to resting mounds have been brought back [36].

In the DMO, the initial HP animals' population of N_{Hp} potential solutions is produced randomly as follows:

$$Hp_k(0) = Hp_{\min} + rand(0,1).\left[Hp_{\max} - Hp_{\min}\right] \quad k = 1, 2, \ldots .N_{Hp} \tag{15}$$

where, Hp_k denotes the position of every HP (k); Hp_{min} and Hp_{max} imply the minimal and highest boundaries. Each HP position is computationally related to the set of the control variables which their number is symbolized by Dim.

Once the HP animals' population of solutions is initialized, the fitness score ($\mathrm{Fit_k}$) of each option (k) is computed. After that, the alpha female (α) is selected as described in Eq. (16) based on the probability worth of each group's fitness.

$$\alpha = \frac{Fit_k}{\sum_{k=1}^{N_{Hp}} Fit_k} \tag{16}$$

The number of HP animals in the alpha party corresponds with the gap between the overall group number (NDM) and the number of babysitters (Bst). Peep is the alpha female's vocalisation, that keeps the HP animals' group on course. Every HP rest inside the initial resting mound that has been allotted to. To construct a prospective food position, the DMO

TABLE 3. Compared algorithms: Parameters and applications.

Algorithm	Ref.	Year	Parameters	Applications
DMO	J. O. Agushaka et al. [36]	2022	• Population size (PS) = 30, • Maximum number of iterations (MNI)= 500 • Number of babysitters = 3 • Alpha female vocalization (peep=2)	generation expansion planning, autoregressive exogenous model identification, detection of diabetic retinopathy, heart disease detection, feature selection for datasets, thermal expansion prediction of Nanocomposites, and frequency regulation with photovoltaic and storage units [38]–[45].
IDMO	Proposed	2023		
AEO	W. Zhao et al. [56]	2020	• PS = 30, • MNI = 500	Reconfiguration of distribution networks [64], groundwater level modeling [65], combined heat and power dispatch [66], path planning for unmanned combat aerial vehicles [67].
AQU	A. H. Abualigah et al. [57]	2021	• PS = 30, • MNI = 500 • Alpha parameter = 0.1 • Delta parameter = 0.1	wind energy potential assessment [68], multiple renewable energy resources in distribution network [69]
EO	A. Faramarzi et al. [58]	2020	• PS = 30, • MNI = 500	Allocation of batteries in distribution systems [70], models of Battery Cells [71], integration of biomass distributed generation in distribution systems [72]
ESMA	S. Sarhan et al. [59]	2022	• PS = 30, • MNI = 500 • z parameter = 0.03	Frequency Stability in Power Systems [73]
GTO	B. Abdollahzadeh et al. [60]	2021	• PS = 30, • MNI = 500	Fuel-cell parameter estimation [74]
RKO	J. Raeisi-Gahruei et al. [61]	2022	• PS = 30, • MNI = 500	Electricity Consumption Prediction [61]
SAA	P. Trojovský et al. [62]	2023	• PS = 30, • MNI = 500	
SMA	S. Li et al. [63]	2020	• PS = 30, • MNI = 500 • z parameter = 0.03	

applies the equation presented in Eq. (17).

$$Hp_k(It+1) = Hp_k(It) + rand(0,1) \times peep, \quad k = 1 : N_{Hp} - Best \tag{17}$$

where It denotes the current iteration. Following every iteration, the resting mound is represented in Eq. (18):

$$SM_k = \frac{Fit_{k+1} - Fit_k}{\max\left(\left|Fit_{k+1} - Fit_k\right|\right)} \tag{18}$$

Eq. (19) provides the mean value (ψ) of the detected resting mound.

$$\psi_k = \frac{\sum_{k=1}^{N_{Hp}} SM_k}{N_{Hp}} \tag{19}$$

When the babysitting transfer condition is met, the DMO technique moves to the scouting step, whenever the next food resource or resting mound is identified. Scouting proceeds simultaneously while foraging in DMO, when the scouts look for a different resting mound, assuring exploring. According to the complete performance of the HP animals, the movement that ensues is shown as an efficient or failure evaluation of constructing a new mound. As in Equation (20), shown at the bottom of the page, may be used to model the scout mongoose, where CF parameter is shown in Eq. (21) and M seems to be a vector that determines the HP animals' migrating to its subsequent resting mound as shown in Eq. (22).

$$CF = \left(1 - \frac{It}{It_{Mx}}\right)^{\left(2 \times It/It_{Mx}\right)} \tag{21}$$

$$M = \sum_{k=1}^{N_{Hp}} \frac{Hp_k \times SM_k}{Hp_k} \tag{22}$$

where It_{Mx} is the maximum number of iterations.

B. PROPOSED IDMO FOR SOLVING THE TCSC ALLOCATION PROBLEM

A novel IDMO utilizing an alpha-directed Learning Process (ADLP) is presented in this part. The creatively recommended treatment incorporates an improved ADLP to improve searching abilities, and the upgrading mechanism is partly led by the adapted alpha. In order to improve the searching capabilities, the ADLP is combined with the

$$Hp_k(It+1) = \begin{cases} Hp_k(It) - CF \times rand(0,1) \times \left(Hp_k(It) - M\right) & if\ \psi_{k+1} > \psi_k \\ Hp_k(It) + CF \times rand(0,1) \times \left(Hp_k(It) - M\right) & Else \end{cases} \quad k = 1, 2, \ldots .N_{Hp} \tag{20}$$

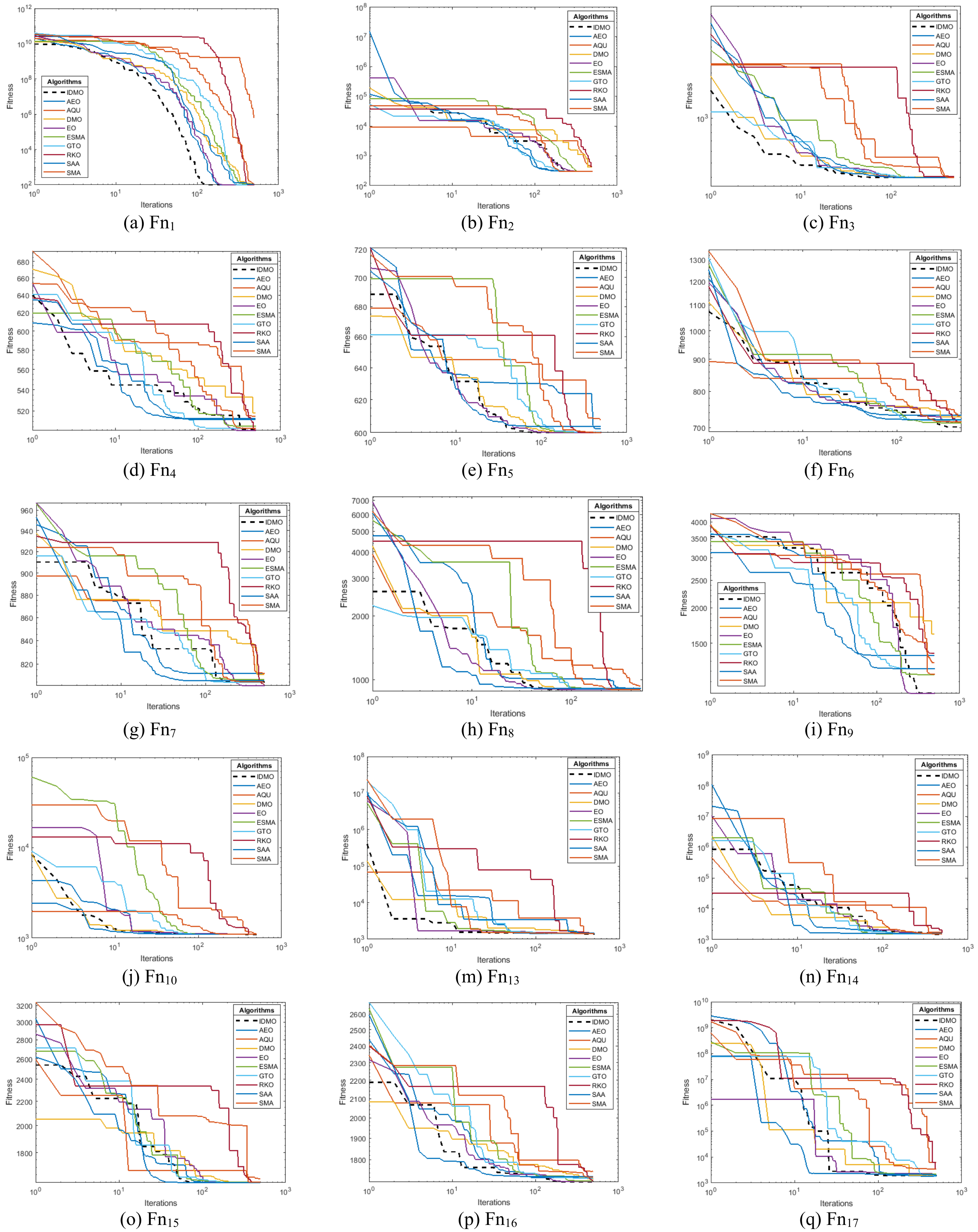

(a) Fn_1 (b) Fn_2 (c) Fn_3
(d) Fn_4 (e) Fn_5 (f) Fn_6
(g) Fn_7 (h) Fn_8 (i) Fn_9
(j) Fn_{10} (m) Fn_{13} (n) Fn_{14}
(o) Fn_{15} (p) Fn_{16} (q) Fn_{17}

FIGURE 3. Convergence properties of IDMO and DMO for CEC 2017 problems.

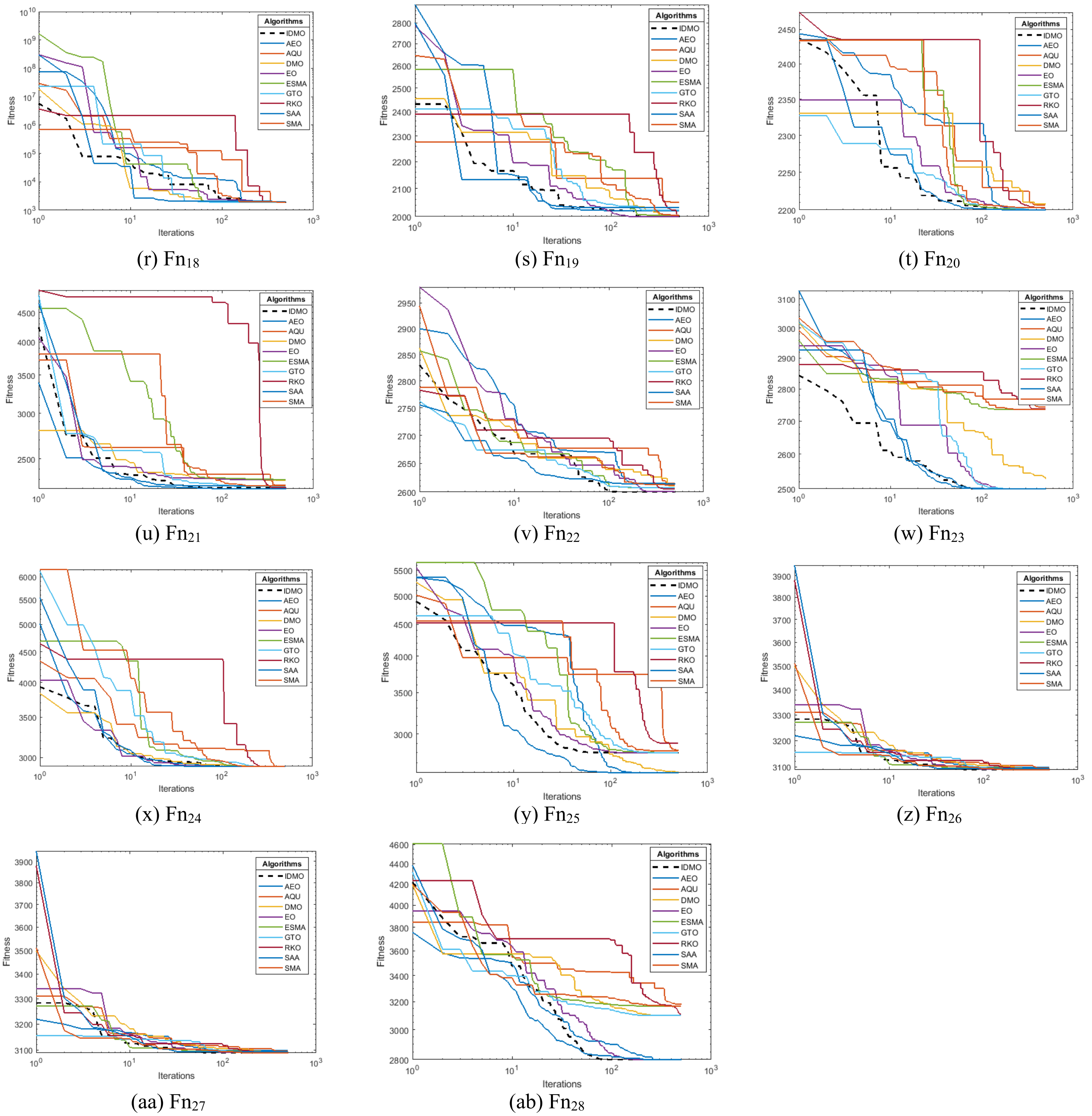

(r) Fn_{18} (s) Fn_{19} (t) Fn_{20}

(u) Fn_{21} (v) Fn_{22} (w) Fn_{23}

(x) Fn_{24} (y) Fn_{25} (z) Fn_{26}

(aa) Fn_{27} (ab) Fn_{28}

FIGURE 3. ***(Continued.)*** **Convergence properties of IDMO and DMO for CEC 2017 problems.**

equation presented in Eq. (17) to create a probable food position. As a result, the location of each seeking solution inside the area of search is enhanced as described as in Eq. (23), shown at the bottom of page 11, where, Hp_{Best} is the alpha position regarding the seeking animal with lowest value of the objective; Hp_{Rd} corresponds to a randomly picked HP animal; and LSV represents the likelihood of selection value. LSV is adjusted to 50% to strike a compromise between the heightened exploitation features given in Eq. (23) and the exploratory qualities indicated in Eq. (17). The exploitative characteristics are significant and powerful though by means of the previously mentioned framework, while the exploratory searching attributes are retained and accomplished through the conventional way at the same time. The essential stages of the IDMO are displayed in Figure 2.

IV. SIMULATION RESULTS

In this part, the application of the proposed IDMO is executed in two directions. At first, simulations of benchmark

TABLE 4. Statistical outcomes of IDMO and DMO for CEC 2017 benchmarking tasks.

No.	Index	IDMO	DMO	AEO	AQU	EO	ESMA	GTO	RKO	SAA	SMA
Fn_1	Best	100.7876	103.1033	101.8204	631630.4	100.1497	**100.3841**	102.2414	101.3583	106.8504	115.6355
	Mean	1833.425	4947.712	2882.311	7117627	**1296.579**	3042.833	3185.564	6394.494	3812.14	**1296.579**
	Worst	10627.66	63834.88	12645.98	47965063	5774.671	5542.366	12581.75	12725.47	12866.27	**5554.671**
	Std	2310.289	12150.27	2748.079	8879770	1727.267	1949.333	3349.887	4340.656	3324.979	**1527.267**
Fn_2	Best	**300**	426.9525	**300**	862.8424	300.0409	300.0009	**300**	301.5553	433.8029	**300**
	Mean	300.005	1075.823	300.0055	14241.48	302.9692	300.0944	**300**	1791.484	1892.281	300.0217
	Worst	300.0741	2487.439	300.1652	78883.29	335.2222	300.3938	**300.0013**	28092.82	20047	300.2815
	Std	0.015802	420.1405	0.024216	17008.76	5.960751	0.094327	**0.000183**	4446.282	2775.047	0.048374
Fn_3	Best	**400.0056**	400.5637	400.1317	402.9141	400.0196	400.011	401.2798	405.4006	403.8382	400.0429
	Mean	**403.1635**	405.2926	404.1969	418.5362	404.718	405.4084	422.5109	450.0849	410.8517	408.777
	Worst	**405.0699**	406.8646	466.8414	576.6982	406.8178	407.2103	481.1919	905.8536	496.1308	476.984
	Std	1.572968	**1.199943**	9.19856	29.72566	1.841029	2.106057	24.41179	78.84186	18.50037	15.8229
Fn_4	Best	502.9849	518.0095	512.9345	514.84	**501.9921**	505.9717	503.9798	502.097	511.9395	503.9838
	Mean	**509.9966**	530.0403	535.6209	528.8363	511.3244	515.6199	525.483	516.5253	535.7457	511.3244
	Worst	521.848	539.6044	559.6972	552.2148	528.8538	**521.4943**	552.7323	543.6022	577.6057	528.8538
	Std	4.927657	5.370918	11.92463	9.884062	5.690601	**3.876852**	10.33986	10.16285	16.49356	5.690601
Fn_5	Best	**600**	**600**	602.2025	607.8623	**600**	600.0447	600.4136	**600**	603.8165	600.0785
	Mean	**600**	**600**	619.4128	616.8517	600.0018	600.0892	607.1628	600.623	617.543	600.0018
	Worst	600.0002	**600.0001**	645.7046	636.7507	600.0396	600.1194	628.7749	617.8881	647.1749	600.0396
	Std	4.1E-05	**1.77E-05**	9.91575	6.212097	0.005762	0.022851	6.537381	2.806871	9.427292	0.005762
Fn_6	Best	**701.9899**	728.6148	733.0717	728.4909	712.062	712.8488	720.3034	714.6422	721.5113	715.2008
	Mean	724.9523	743.0721	764.578	760.7281	**722.8181**	724.8084	751.6431	734.864	751.7038	722.8181
	Worst	750.1594	753.9905	809.9773	812.3142	738.97	**731.801**	787.9011	761.6374	791.7054	738.97
	Std	10.17492	5.371381	19.37887	18.5329	5.659119	**5.107153**	15.84439	12.40402	18.37205	5.659119
Fn_7	Best	804.9748	811.2899	811.9395	812.173	**801.99**	806.9651	804.9748	803.0511	805.9697	804.9792
	Mean	**811.3417**	829.6501	830.2268	828.0318	812.1872	814.5285	827.3158	813.5723	822.3442	812.1872
	Worst	826.8638	841.7104	862.682	846.8473	824.0725	**820.8969**	841.5043	837.339	841.7882	824.0725
	Std	4.85141	6.106073	13.06553	7.133653	4.290194	**4.193956**	8.150514	9.903987	7.530569	4.290194
Fn_8	Best	**900**	**900**	912.7674	935.9179	**900**	900.0002	902.6364	**900**	910.5194	900.0007
	Mean	900.0218	**900**	1062.502	1080.06	900.2292	900.0015	951.3241	900.9298	1080.856	900.2292
	Worst	900.4543	**900**	1312.112	1358.738	901.8173	900.003	1195.189	918.829	1895.92	901.8173
	Std	0.090935	**2.53E-09**	105.2	93.07999	0.471233	0.000835	64.66907	2.873668	170.4958	0.471233
Fn_9	Best	1003.665	1615.589	1361.636	1282.538	**1000.188**	1165.269	1224.032	1382.47	1221.682	1168.721
	Mean	1528.554	2276.483	2044.173	1898.988	1505.309	**1462.236**	2005.585	1809.26	2024.885	1505.309
	Worst	2498.384	3533.997	2702.938	2405.251	2058.839	**1679**	2757.256	2535.195	3318.621	2058.839
	Std	406.6325	277.9387	315.3252	239.4575	271.8187	**146.268**	309.5439	324.4173	370.4943	271.8187
Fn_{10}	Best	**1100.35**	1103.032	1104.978	1126.013	1101.077	1101.012	1103.123	1101.18	1103.253	1103.395
	Mean	**1104.631**	1107.101	1142.565	1245.853	1107.331	1112.406	1136.846	1152.762	1158.702	1107.331
	Worst	**1113.661**	1112.527	1225.362	1543.506	1122.641	1124.254	1474.95	1361.733	1273.258	1122.641
	Std	**2.989418**	2.507902	26.48832	95.9905	4.106186	6.674326	52.57824	85.62553	43.42037	4.106186
Fn_{11}	Best	**1215.061**	7581.318	1468.727	59003.65	2401.326	3253.422	2251.604	11046.39	2220.099	5561.43
	Mean	17608.6	147990.2	16070.97	5839942	**9346.397**	213446.9	19484.78	556267.5	16173.04	9346.397
	Worst	55835.9	848651.8	49512.6	21294607	31534.92	597806.4	52538.98	15705336	53781.33	**30534.92**
	Std	14061.98	157984.9	13360.44	6235390	6211.869	189660.3	14651.39	2309722	13805.32	**6201.869**
Fn_{12}	Best	**1309.993**	1471.087	1359.1	2983.547	1338.598	1319.615	1301.353	1596.162	1521.598	1465.071
	Mean	5704.653	4806.373	**1902.443**	16104.91	7758.507	2161.825	1661.761	12489.74	11073.28	7758.507
	Worst	20603.37	14058.03	7881.334	57140.58	22741.2	**4041.885**	2445.92	72354.44	36272.32	22741.2
	Std	4845.41	2962.256	1146.132	11977.37	6177.924	**647.7571**	301.6881	11704.68	9503.086	6177.924
Fn_{13}	Best	**1405.386**	1437.532	1421.297	1475.86	1436.545	1434.14	1413.99	1468.283	1451.43	1435.026
	Mean	**1437.81**	93986408	1460.401	2726.689	1472.594	1764.307	1461.535	1594.974	3218.386	1472.594
	Worst	**1519.64**	3.81E+09	1602.707	7300.955	1584.345	2503.962	1513.531	2492.51	14794.43	1584.345
	Std	**25.11236**	5.51E+08	30.65953	1181.206	26.43559	326.2715	27.67236	161.0686	2633.219	26.43559
Fn_{14}	Best	**1501.567**	1574.339	1511.757	1704.87	1528.837	1504.672	1503.209	1666.848	1562.425	1522.306
	Mean	1607.876	1894.31	1590.464	7155.795	1781.199	4320.751	**1586.639**	2545.096	3284.562	1781.199
	Worst	1983.927	2742.553	2787.242	13013.25	3504.08	7356.117	**1860.807**	4767.804	5926.97	3504.08
	Std	122.1004	289.9846	179.6528	2819.584	337.9089	1898.652	**74.26103**	803.5599	1216.997	337.9089
Fn_{15}	Best	**1600.168**	1601.544	1601.514	1625.733	1600.752	1601.818	1601.468	1600.854	1601.703	1602.053
	Mean	1618.608	**1613.991**	1756.826	1799.318	1653.25	1646.452	1700.231	1632.426	1817.625	1653.25
	Worst	1733.113	1738.793	2010.423	2117.308	1855.858	**1731.645**	1992.801	1900.84	2135.552	1855.858
	Std	**42.59626**	22.69649	136.1562	128.3401	84.77303	45.34023	95.75652	58.07911	142.0484	84.77303
Fn_{16}	Best	**1700.44**	1712.647	1718.391	1745.723	1702.668	1705.451	1716.933	1706.86	1723.965	1720.961
	Mean	**1716.586**	1740.727	1771.682	1781.167	1730.943	1730.1	1742.867	1742.974	1783.957	1730.943
	Worst	1783.647	1761.893	1898.971	1858.912	1795.37	**1747.782**	1800.339	1781.586	1925.583	1795.37
	Std	17.16368	9.774917	39.24548	26.89721	19.93134	**12.02978**	16.51172	11.82739	53.54611	19.93134
Fn_{17}	Best	1926.524	1983.072	**1839.184**	6124.661	2247.015	2166.893	1849.487	3489.732	1990.645	3473.383
	Mean	9969.52	7055.869	**4711.676**	45811.23	11821.5	24255.66	4734.006	33008.39	10866.06	11821.5

TABLE 4. ***(Continued.)*** **Statistical outcomes of IDMO and DMO for CEC 2017 benchmarking tasks.**

	Worst	31100.49	**19019.33**	20898.85	72733.15	34209.1	35618.39	34251.62	209371	55426.05	34209.1
	Std	7118.979	**4063.737**	4337.082	15609.74	8429.008	9720.003	6545.115	34519.64	11000.98	8429.008
Fn_{18}	Best	**1902.787**	1911.531	1904.357	2007.858	1916.638	1915.654	1904.802	1947.243	2025.102	1908.044
	Mean	1984.067	2172.458	**1943.842**	25488.55	2783.073	3553.279	1963.373	3129.286	11852.15	2783.073
	Worst	2560.898	3884.533	2176.958	120047.6	12165.36	13985.14	**2095.158**	9117.7	208941.3	12165.36
	Std	114.2122	328.5189	47.23035	21289.85	1954.927	2695.933	**53.05017**	1670.582	28897.4	1954.927
Fn_{19}	Best	**2000**	2000.323	2021.307	2049.27	2000.312	2004.049	2021.732	2001.065	2031.366	2005.325
	Mean	**2002.347**	2010.275	2089.448	2134.692	2021.964	2021.755	2092.222	2040.972	2146.249	2021.964
	Worst	**2017.46**	2035.596	2253.704	2262.899	2140.046	2036.477	2206.172	2161.175	2324.983	2140.046
	Std	**3.165724**	10.40192	54.23813	56.72375	31.21513	10.29943	53.84462	48.08278	74.54465	31.21513
Fn_{20}	Best	**2200**	2207.963	**2200**	2206.064	2200.033	2200.035	**2200**	2202.68	**2200**	2202.781
	Mean	2241.143	2421.83	2233.399	2303.841	2296.691	2313.871	**2217.228**	2269.041	2311.109	2296.691
	Worst	2317.597	3423.376	2347.792	2348.035	2323.166	2328.945	2342.25	2341.668	2379.046	**2323.166**
	Std	53.15606	276.8203	57.32245	49.8612	39.24597	**31.07273**	43.09881	59.03082	53.57661	39.24597
Fn_{21}	Best	2224.237	2290.772	**2215.181**	2245.189	2300	2300.512	2237.236	2225.953	2244.561	2241.042
	Mean	**2298.119**	2302.682	2305.617	2310.746	2300.585	2301.876	2303.812	2395.433	2309.082	2300.585
	Worst	2302.433	2306.795	2361.027	2331.133	**2301.545**	2302.875	2319.036	3882.778	2345.843	2301.545
	Std	14.81279	2.544353	18.1344	14.20948	**0.430805**	0.649297	10.3266	333.9873	12.51222	0.430805
Fn_{22}	Best	**2600**	2611.39	2614.973	2614.735	2600.529	2607.424	2607.767	2605.674	2614.191	2612.391
	Mean	**2612.981**	2626.133	2651.285	2639.714	2613.545	2616.508	2623.589	2628.164	2655.502	2613.545
	Worst	2628.926	2643.387	2724.523	2680.313	2629.856	**2623.644**	2683.03	2712.256	2714.223	2629.856
	Std	5.582052	7.061391	26.47565	13.18305	6.756141	**4.604779**	13.03785	25.15645	25.23442	6.756141
Fn_{23}	Best	**2500**	2529.358	**2500**	2743.333	**2500**	2735.422	**2500**	2737.125	**2500**	2734.674
	Mean	2702.739	2779.46	**2694.044**	2765.077	2723.141	2750.97	2722.229	2760.733	2776.754	2723.141
	Worst	2756.668	4667.793	2858.199	2791.924	2748.113	2762.685	2785.801	2862.941	2881.822	**2748.113**
	Std	89.56668	403.3049	126.3004	11.60206	57.12793	7.401766	91.37158	25.74767	48.65351	**57.12793**
Fn_{24}	Best	**2897.746**	2898.008	2897.762	2898.884	2897.762	2897.835	2897.757	2897.94	2897.941	2898.208
	Mean	2927.649	2923.861	2929.203	2938.885	2923.014	2917.771	2928.394	2928.859	2927.008	**2923.014**
	Worst	2948.79	**2945.222**	2957.215	3030.515	2949.895	2947.002	2971.013	2953.657	2978.515	2949.895
	Std	22.86882	**20.46398**	23.68665	27.90755	23.50277	23.58085	25.28154	24.11888	25.58298	23.50277
Fn_{25}	Best	2800	**2606.09**	2600	2825.635	2800	2800.154	2800	2900	2600	2816.011
	Mean	2903.254	**2865.906**	3030.664	3020.676	2885.049	2953.345	2984.508	3165.254	3132.256	2885.049
	Worst	2959.341	**2900.003**	3461.777	3489.538	2958.158	2999.128	3207.704	4028.093	4234.516	2958.158
	Std	**28.02168**	56.84354	155.2969	153.5662	42.05265	46.95114	99.90624	384.0885	363.1331	42.05265
Fn_{26}	Best	3090.001	3091.548	3098.815	3095.366	3091.967	**3089.013**	3090.752	3089.308	3093.179	3089.031
	Mean	3095.652	3095.589	3126.583	3100.941	3099.475	**3091.03**	3101.365	3099.07	3129.619	3099.475
	Worst	3103.205	3100.03	3233.854	3116.125	3171.966	**3092.688**	3198.189	3197.703	3209.53	3171.966
	Std	2.793392	1.944856	31.32213	4.757791	11.537	**1.184862**	19.81815	18.70578	36.35269	11.537
Fn_{27}	Best	**2800**	3100	2800.001	3182.341	**2800**	3166.526	3100	3108.935	2800.009	3167.467
	Mean	**3187.874**	3191.247	3252.369	3379.829	3261.622	3342.206	3289.245	3352.853	3277.773	3261.622
	Worst	3444.132	**3411.823**	3446.527	3499.317	3446.483	3411.823	3783.223	3731.813	3412.053	3446.483
	Std	143.5352	88.55182	154.9652	**83.32384**	161.7679	102.4616	187.6894	193.3343	147.9899	161.7679
Fn_{28}	Best	3141.97	3186.272	3183.416	3153.017	3144.619	**3134.422**	3147.311	3138.465	3161.176	3134.366
	Mean	3183.661	3223.056	3264.007	3234.006	3192.803	3180.666	3219.908	**3175.727**	3271.415	3192.803
	Worst	3273.349	3265.67	3403.968	3332.945	3302.278	3235.338	3397.49	**3234.517**	3424.743	3302.278
	Std	20.41437	**16.49242**	53.20727	43.72574	33.45711	32.19293	58.00608	24.26783	65.41059	33.45711

functions are implemented considering CEC 2017 single objective optimization competition with comparison to several recent metaheuristic algorithms. Second, simulations are conducted in solving the TCSC allocation problems in power networks considering two IEEE standard power systems of 30 and 57 buses.

A. APPLICATION ASSESSMENT FOR CEC 2017 BENCHMARKING MODELS

Due to the lack of a formal proof, it can be difficult to determine the amount of "good" of an effective optimisation strategy; therefore, benchmarking functions provide an important role in evaluating the usefulness of these strategies. As a consequence, the proposed IDMO and DMO techniques' performance is evaluated in this work utilizing the CEC 2017 competition as a benchmark [55]. This test provides a number of routines for checking different attributes. Unimodal, multimodal, mixed, and composite functions are among those explored. Table 2 shows those unrestricted benchmarking functions. For all the 28 benchmarking functions, the considered dimension is 30 control variables while their bounds are [−100,100].

$$Hp_k(It+1) = \begin{cases} Hp_{Best}(It) + rand(0,1) \times \left(Hp_k(It) - Hp_{Rd}(It)\right) & \text{if rand} < \text{LSV} \\ Hp_k(It) + rand(0,1) \times peep & Else \end{cases} \quad k = 1, 2, ..N_{Hp} - Best \tag{23}$$

TABLE 5. Ranking by Friedman of the comparing algorithms' average objective values for the CEC 2017 problems.

Task	IDMO	DMO	AEO	AQU	EO	ESMA	GTO	RKO	SAA	SMA
Fn_1	3	8	4	10	**1.5**	5	6	9	7	**1.5**
Fn_2	2	8	3	9	6	5	**1**	10	4	7
Fn_3	**1**	5	2	10	3	6	7	9	8	4
Fn_4	**1**	8	9	7	2	4	6	5	10	3
Fn_5	**1.5**	**1.5**	10	8	3	5	7	6	9	4
Fn_6	4	6	10	9	**1**	3	7	5	8	2
Fn_7	**1**	9	10	8	2	5	7	4	6	3
Fn_8	3	**1**	8	9	4	2	7	6	10	5
Fn_9	4	10	9	6	2	**1**	7	5	8	3
Fn_{10}	**1**	2	7	10	3	5	6	8	9	4
Fn_{11}	5	7	3	10	**1**	8	6	9	4	2
Fn_{12}	5	4	2	10	6	3	**1**	9	8	7
Fn_{13}	**1**	10	2	8	4	7	3	6	9	5
Fn_{14}	3	6	2	10	4	9	**1**	7	8	5
Fn_{15}	2	**1**	8	9	5	4	7	3	10	6
Fn_{16}	**1**	5	8	9	3	2	6	7	10	4
Fn_{17}	4	3	**1**	10	6	8	2	9	5	7
Fn_{18}	3	4	**1**	10	5	8	2	7	9	6
Fn_{19}	**1**	2	7	9	4	3	8	6	10	5
Fn_{20}	3	10	2	7	5	9	**1**	4	8	6
Fn_{21}	**1**	5	7	9	2	4	6	10	8	3
Fn_{22}	**1**	6	9	8	2	4	5	7	10	3
Fn_{23}	2	10	**1**	8	4	6	3	7	9	5
Fn_{24}	6	4	9	10	2	**1**	7	8	5	3
Fn_{25}	4	**1**	8	7	2	5	6	10	9	3
Fn_{26}	3	2	9	7	5	**1**	8	4	10	6
Fn_{27}	**1**	2	3	10	4	8	7	9	6	5
Fn_{28}	3	7	9	8	4	2	6	**1**	10	5
Summation	**70.5**	147.5	163	245	95	133	146	190	227	122
Mean rank	**2.517857**	5.267857	5.821429	8.75	3.392857	4.75	5.214286	6.785714	8.107143	4.357143
Final Ranking	**1**	6	7	10	2	4	5	8	9	3
Improvement %	-	52.20%	56.75%	71.22%	25.79%	46.99%	51.71%	62.89%	68.94%	42.21%

The suggested IDMO is carried out in contrast to the traditional DMO, with the CEC 2017 single objective optimization criteria, which are shown in Table 2, taken into account. Also, several recent optimization techniques are taken into contrast including artificial ecosystem optimization (AEO) [56], aquila optimization (AQU) [57], equilibrium optimization (EO) [58], enhanced slime mould algorithm (ESMA) [59], Gorilla troops optimization (GTO) [60], red kite optimization (RKO) [61], subtraction-average-based algorithm (SAA) [62] and slime mould algorithm (SMA) [63]. In relation to the contrasted techniques, Table 3 shows their necessary settings and a number of effective applications. Fifty different operations based on each method for every benchmark have been looked at to eliminate the impact of randomness.

Based on the circumstances stated in Table 3, the compared algorithms are applied for the CEC 2017 benchmarks that are described in Table 2. Fig. 3 displays the convergence features of the DMO, IDMO, AEO, AQU, EO, ESMA, GTO, RKO, SAA and SMA, respectively. In similar time, Table 4 depicts the regarding statistical metrics in terms of the best, mean, worst and standard deviation (Std) outcomes. As shown in Table 4, the introduced IDMO technique demonstrates the best strength by attaining the least statistical indices in most of the benchmark functions. As shown:

- Compared to the standard DMO, the IDMO shows improvement of 96.43%, 71.43%, 60.71% and 46.43%, accordingly regarding the best, mean, worst and Std.

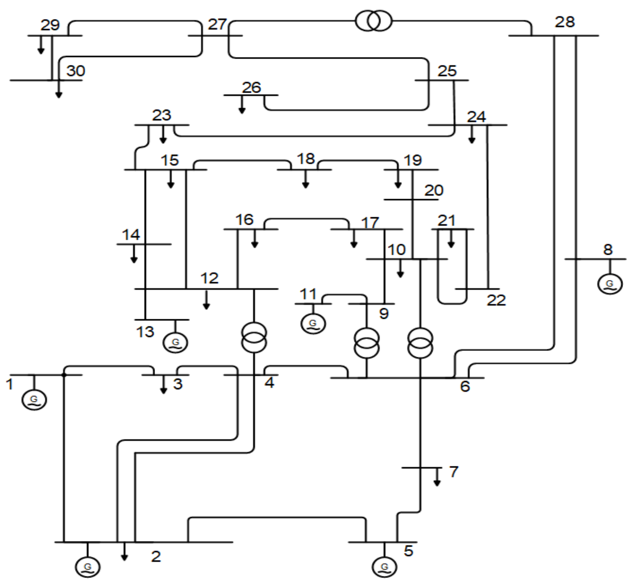

FIGURE 4. Line-diagram of the first power system [77].

- Compared to the AEO, the proposed IDMO derives improvement of 89.29%, 75.00%, 85.71% and 82.14%, accordingly.
- Compared to the AQU, the proposed IDMO acquires improvement of 100.00%, 100.00%, 96.43% and 82.14%, respectively.

TABLE 6. Outcomes of the compared algorithms for TCSC device allocations regarding Case 1.

	Initial Case	AQU	GWO	AEO	SAA	DMO	IDMO
VG 1	1.0500	1.1000	1.099568	1.099351	1.1000	1.077325	1.0997
VG 2	1.0400	1.1000	1.095818	1.094747	1.09755	1.07729	1.097107
VG 5	1.0100	1.09728	1.08001	1.074308	1.079716	1.05654	1.078474
VG 8	1.0100	1.09288	1.085785	1.083873	1.08684	1.066889	1.084998
VG 11	1.0500	1.1000	1.078706	1.099959	1.1000	1.097459	1.099309
VG 13	1.0500	1.1000	1.081997	1.099709	1.1000	1.089488	1.099962
Ta 6-9	1.0780	1.1000	1.025412	1.028284	1.067173	0.979025	1.023229
Ta 6-10	1.0690	0.910477	0.961107	0.925326	0.9000	0.94149	0.937607
Ta 4-12	1.0320	1.009181	1.008998	0.999935	0.986297	0.973187	0.983766
Ta 28-27	1.0680	1.034419	1.00225	0.98665	0.973996	0.968219	0.976997
Qr 10	0.000	5.000	2.13309	4.152465	5.000	2.041835	4.453243
Qr 12	0.000	3.962959	3.124115	4.930084	5.000	3.90699	4.760074
Qr 15	0.000	5.000	0.258411	4.952519	4.999997	4.341322	4.095576
Qr 17	0.000	5.000	3.793636	4.912524	4.999982	4.602435	4.995081
Qr 20	0.000	5.000	2.796705	1.71465	4.081398	3.530735	4.461134
Qr 21	0.000	5.000	4.209032	4.899575	4.968112	4.89273	4.973731
Qr 23	0.000	4.881004	3.763496	0.885251	2.58453	3.418359	2.662936
Qr 24	0.000	5.000	3.481095	3.534451	5.000	4.364901	4.941651
Qr 29	0.000	3.107001	2.864193	2.708482	2.275642	1.892259	2.560601
PG 1	99.2400	51.3952	62.3303	51.4936	51.21077	52.61437	51.33157
PG 2	80.000	80.000	79.61742	79.78346	80.000	79.5501	79.97828
PG 5	50.000	50.000	49.8189	49.86303	50.000	49.83164	49.99382
PG 8	20.000	35.000	33.99505	34.99899	35.000	34.71168	34.94736
PG 11	20.000	30.000	29.7921	29.55887	30.000	29.72535	29.98847
PG 13	20.000	40.000	37.77225	39.98309	40.000	39.98591	39.97617
TCSC location	-	6-28	4-6	28-27	28-27	10-17	28-27
TCSC Compensation	-	-42.017%	-35.028%	-49.490%	-49.998%	-11.44%	-49.72%
Losses (MW)	5.832400	2.990	3.035	2.844	2.8217	3.019	**2.81565**

Positive and negative indications represent an increase or decrease in the transmission line reactance connected with TCSC, respectively.

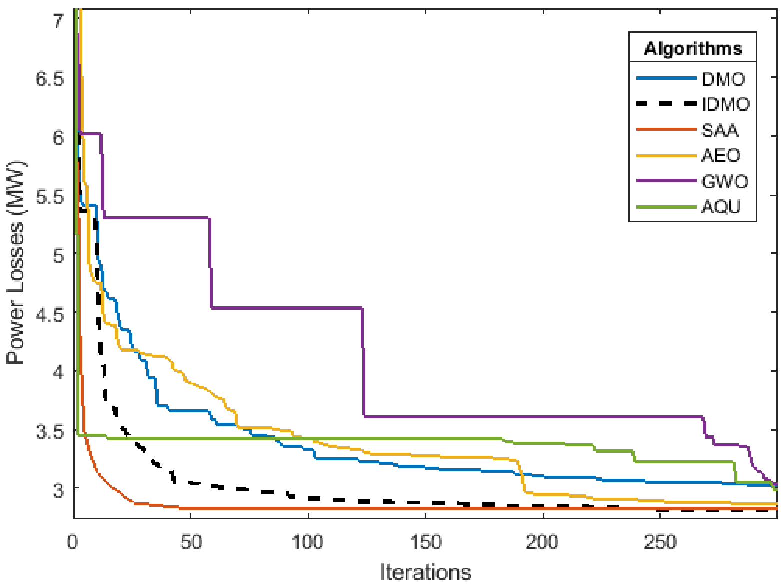

FIGURE 5. Implemented algorithms' convergence curves regarding Case 1.

- Compared to the EO, the IDMO shows improvement of 85.71%, 78.57%, 71.43% and 71.43%, accordingly.
- Compared to the ESMA, the proposed IDMO achieves improvement of 89.29%, 75.00%, 50.00% and 50.00%, respectively.

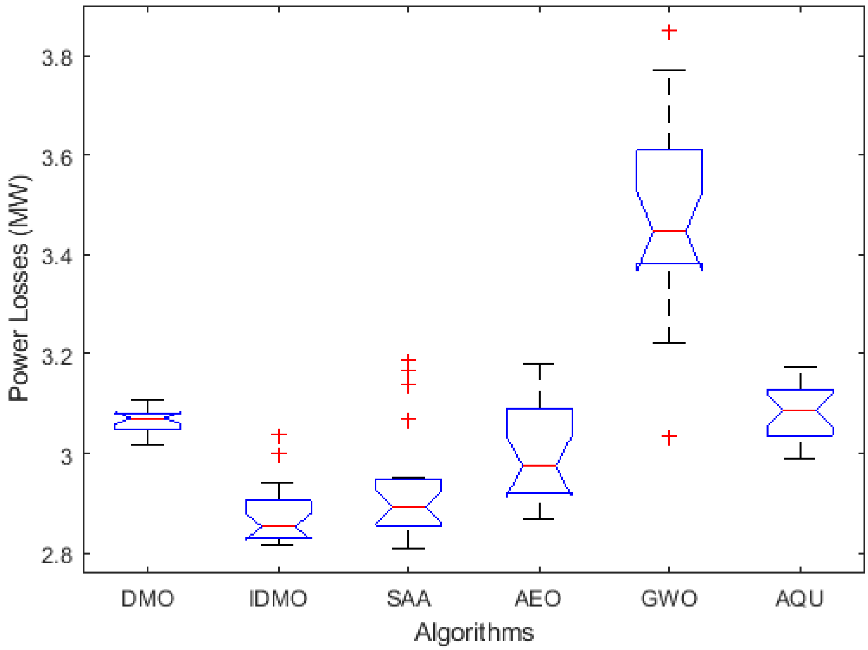

FIGURE 6. Box plot related to the Outcomes of the compared algorithms for Case 1.

TABLE 7. Statistical outcomes of the obtained Losses (MW) for Case 1.

	DMO	IDMO	SAA	AEO	GWO	AQU
Best	3.019	2.816	2.8217	2.867	3.035	2.990
Mean	3.065	2.875	2.930	3.007	3.472	3.080
Worst	3.109	3.038	3.188	3.180	3.849	3.172
STD	0.026	0.061	0.117	0.100	0.200	0.057
Time*	0.673	0.688	0.511	0.925	0.721	0.954

Time indicates the average time per iteration measured in seconds.

- Compared to the GTO, the proposed IDMO finds improvement of 92.86%, 78.57%, 78.57% and 67.86%, accordingly.
- Compared to the RKO, the proposed IDMO obtains improvement of 82.14%, 96.43%, 92.86% and 89.29% %, respectively.
- Compared to the SAA, the proposed IDMO attains improvement of 96.43%, 92.86%, 92.86% and 85.71%, accordingly.
- Compared to the SMA, the proposed IDMO provides improvement of 92.86%, 78.57%, 71.43% and 71.43%, respectively.

Additionally, for the benchmarking task functions of the CEC 2017, Table 5 records the outcomes of a Friedman ranking test related to the proposed IDMO, the basic DMO [36] (2020), AEO [56] (2020), AQU [57] (2021), EO [58] (2020), ESMA [59] (2022), GTO [60] (2021), RKO [61] (2022), SAA [62] (2023) and SMA [63] (2020), respectively. As shown, the designed IDMO achieves the least average rank of 2.517 achieving the superior outcomes by obtaining the first rank. In the second level, the EO accomplishes a mean rank of 3.3928 while the SMA realizes the third level by 4.357. Also, ESMA, GTO and the standard DMO comes in the fourth, fifth and sixth order, respectively with mean ranks of 4.75, 5.214 and 5.267. Furthermore, AEO, RKO and SAA come in the fourth, fifth and sixth order, respectively with mean ranks of 8.82, 6.785 and 8.107 while AQU shows the worst performance with mean rank of 8.75. Based on these results, the proposed IDMO shows improvement reduction of 25.79%, 42.21%, 46.99%, 51.71%, 52.20%, 56.75%, 62.89%, 68.94% and 71.22% in comparison to EO, SMA, ESMA, GTO, DMO, AEO, RKO, SAA and AQU, respectively.

B. APPLICATIONS FOR TCSC ALLOCATIONS IN IEEE STANDARD 30-BUS TRANSMISSION NETWORK

In this section, the IEEE standard 30-bus system, shown in Fig. 4 [75], is utilized to handle the optimal TCSC allocations. This system includes 41 lines, 30 nodes, 4 transformers, and 9 compensators [76]. The maximum generator voltage 1.10 p.u. and the corresponding tap positions is 0.90 p.u. For the load buses, the voltage limits are 1.05 and 0.95 p.u., these limits for the generator bus are 1.10 and 0.90 p.u., respectively. The IDMO is contrasted with DMO and other recent algorithms of AQU, GWO, AEO and SAA. For all implemented algorithms, 20 times are separately executed where the number of iterations and searching individuals are taken of 300 and 50, respectively. They are performed. Based on the number of the candidate allocated TCSC devices, three disparate cases are investigated considering one, two and three devices.

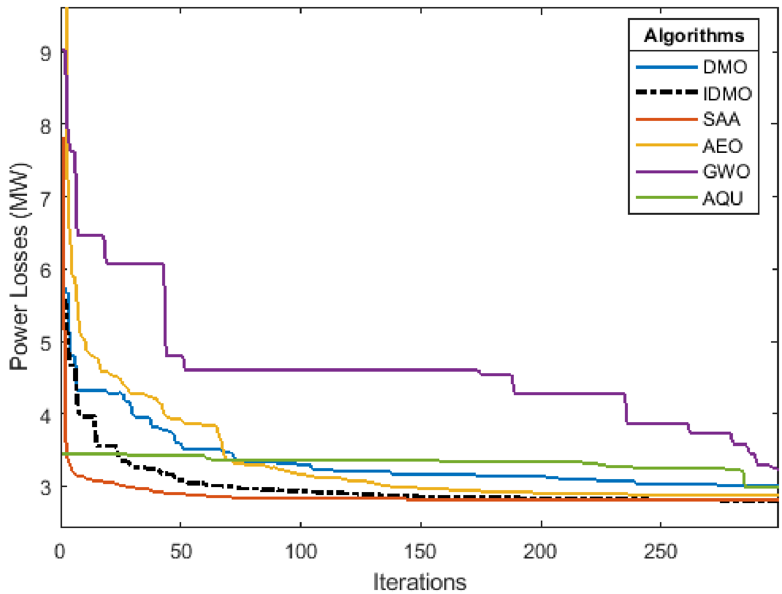

FIGURE 7. Implemented algorithms' convergence curves regarding Case 2.

TABLE 8. Outcomes of the compared algorithms for TCSC device allocations regarding Case 2.

	Initial Case	AQU	GWO	AEO	SAA	DMO	IDMO
VG 1	1.0500	1.1	1.095119	1.099352	1.1	1.088672	1.09986
VG 2	1.0400	1.1	1.089415	1.096829	1.097584	1.084124	1.095882
VG 5	1.0100	1.1	1.071614	1.078726	1.079817	1.063908	1.077982
VG 8	1.0100	1.094221	1.078618	1.086607	1.087006	1.076237	1.084631
VG 11	1.0500	1.1	1.084584	1.099927	1.1	1.098864	1.099862
VG 13	1.0500	1.1	1.074647	1.099558	1.1	1.079165	1.09972
Ta 6-9	1.0780	1.044803	1.049704	0.976591	1.064807	0.973169	1.051505
Ta 6-10	1.0690	0.929538	1.032416	1.016372	0.900035	1.004953	0.915569
Ta 4-12	1.0320	1.011769	1.063337	1.00762	0.980145	0.986186	0.985467
Ta 28-27	1.0680	1.023534	1.002449	0.994596	0.980535	0.974498	0.970748
Qr 10	0	5	3.497458	4.482774	5	1.238543	4.624782
Qr 12	0	5	0.832066	3.665279	5	3.739474	4.991793
Qr 15	0	4.987603	4.166941	3.945993	0	4.203835	4.625295
Qr 17	0	5	3.173012	4.659533	5	2.920776	4.873148
Qr 20	0	4.879124	0.851722	4.934657	5	4.001807	4.231455
Qr 21	0	5	3.394242	2.590238	4.999997	4.127666	4.976453
Qr 23	0	5	1.978594	2.648497	4.274824	3.891986	2.761689
Qr 24	0	5	1.815333	4.935695	5	4.158987	4.887319
Qr 29	0	5	0.977867	2.42653	2.352175	1.801884	2.027743
PG 1	99.2400	51.39525	62.3303	51.49365	51.18843	53.22761	51.28323
PG 2	80	80	72.62864	79.80634	80	79.01535	79.94034
PG 5	50	50	49.966	49.99955	49.99428	49.82904	49.9956
PG 8	20	35	32.48052	34.98885	35	34.8643	34.9966
PG 11	20	30	29.75128	29.99324	30	29.8851	29.99234
PG 13	20	40	39.47006	39.98501	40	39.58471	39.99446
First TCSC installed Lines	-	10-17	6-8	6-9	28.27	10-21	4-12
First TCSC Compensation	-	-13.64%	24.83%	16.10%	-50.00%	-13.52%	49.78%
Second TCSC installed Lines	-	6-28	16-17	4-12	6-28	15-23	2-5
Second TCSC Compensation	-	-44.06%	-2.74%	49.90%	-50.00%	23.10%	-25.01%
Losses (MW)	5.832400	2.995	3.227	2.867	2.820	3.006102	2.802571

Positive and negative indications represent an increase or decrease in the transmission line reactance connected with TCSC, respectively.

1) CASE 1

The allocation of one TCSC device is optimized in this case to get the minimum power losses using the proposed IDMO. The obtained results are compared with DMO, SAA, AEO, AQU, and GWO.

Table 6 shows the optimal control variables which are the generators voltage and output power, the Var sources

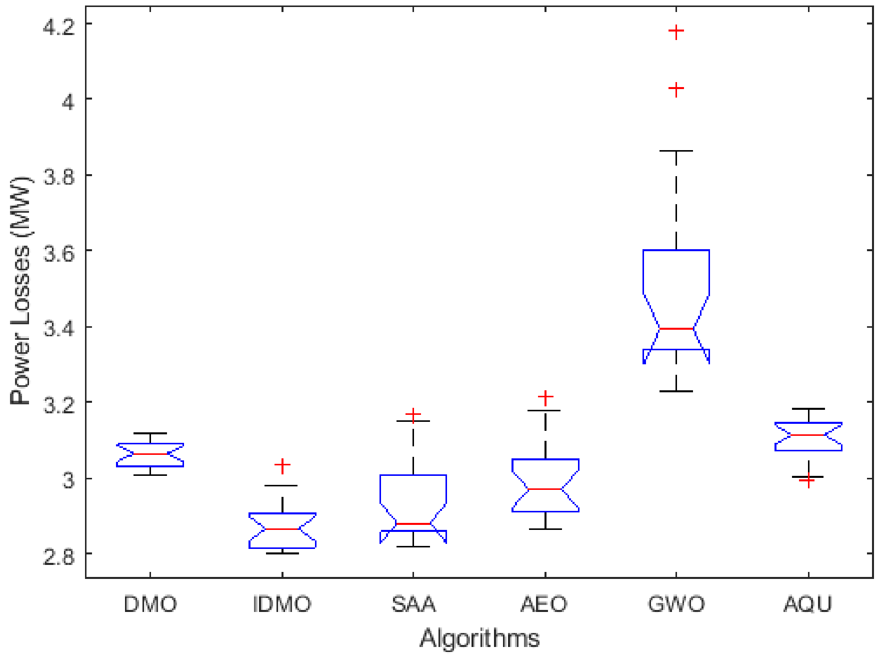

FIGURE 8. Box plot related to the outcomes of the compared algorithms for Case 2.

injection power and the tap value besides the placement and sizing of the TCSC device. Furthermore, the proposed IDMO, standard DMO, AEO, AQU, and GWO converging curves are shown in Fig. 5. As demonstrated, the proposed IDMO produces the lowest power losses of 2.8156 MW. The proposed IDMO gets the transmission line (28-27) as best location of TCSC with 49.72% subtraction in sizing from the installed line reactance. The proposed IDMO attained a 51.72% reduction in power losses when compared with the initial case. When comparing the results of the proposed IDMO with the standard DMO, the proposed IDMO accomplishes a significant reduction percentage of 6.74% in the power losses. Also, the proposed IDMO achieves a 5.83% reduction in the power losses compared with the AQU. Likewise, the proposed IDMO achieves a 7.23% reduction compared to GWO. Furthermore, the proposed IDMO achieves a nearly 1% reduction percentage compared to the obtained results by the AEO and SAA.

TABLE 9. Statistical outcomes of the obtained Losses (MW) for Case 2.

	DMO	IDMO	SAA	AEO	GWO	AQU
Best	3.006	2.803	2.820	2.867	3.227	2.995
Mean	3.063	2.873	2.938	2.988	3.501	3.105
Worst	3.119	3.034	3.168	3.214	4.180	3.181
STD	0.033	0.063	0.112	0.103	0.266	0.053
Time*	0.681	0.698	0.524	0.951	0.749	0.972

Time indicates the average time per iteration measured in seconds.

Fig. 6 shows the box plot associated with the results of the compared algorithms for Case 1 in order to perform a statistical assessment of the compared procedures. Table 7 displays the associated statistical outcomes of the obtained Losses (MW) for this case. It is evident that by aggregating the fewest indices from the obtained objective values, the proposed IDMO works best. In terms of average acquired losses, DMO, SAA, AEO, GWO, and AQU receive losses of 3.065, 2.930, 3.007, 3.472, and 3.080 MW, respectively, while the suggested IDMO finds the lowest losses of 2.875 MW. In comparison to the results achieved by the DMO, SAA, AEO, GWO, and AQU, the suggested IDMO achieves improvement reductions of 6.22%, 1.87%, 4.39%, 17.20%, and 6.67%, respectively. The suggested IDMO finds the lowest losses, 3.038 MW, based on the worst obtained losses, whereas DMO, SAA, AEO, GWO, and AQU receive losses, 3.109, 3.188, 3.180, 3.849, and 3.172 MW, respectively. In comparison to the findings achieved by the DMO, SAA, AEO, GWO, and AQU, the suggested IDMO achieves improvement reductions of 2.29%, 4.71%, 4.46%, 21.08%, and 4.23%, respectively. Table 7 provides the computation burden, measured as the average time per iteration as well.

2) CASE 2

The allocations of two TCSC devices are optimized in this case to get the minimum power losses using the proposed IDMO. Table 8 shows the optimal control variables related to the proposed IDMO, standard DMO, AEO, SAA, AQU, and GWO where the corresponding convergences are displayed in Fig. 7. As demonstrated, the IDMO outputs the lowest power losses of 2.802 MW. The proposed IDMO selects the

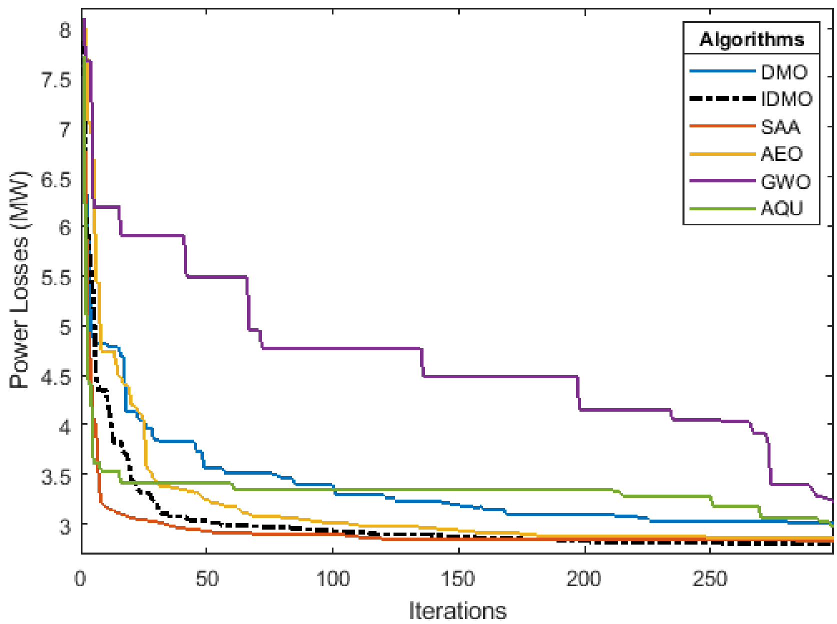

FIGURE 9. Implemented algorithms' convergence curves regarding Case 3.

TABLE 10. Outcomes of the compared algorithms for TCSC device allocations regarding Case 3.

	Initial Case	AQU	GWO	AEO	SAA	DMO	IDMO
VG 1	1.0500	1.097922	1.086747	1.099981	1.1	1.086175	1.098742
VG 2	1.0400	1.097226	1.082197	1.095393	1.1	1.081437	1.094726
VG 5	1.0100	1.082092	1.061782	1.076605	1.082327	1.060443	1.076291
VG 8	1.0100	1.091701	1.068615	1.083436	1.08939	1.065392	1.08014
VG 11	1.0500	1.095909	1.081636	1.088431	1.1	1.096995	1.097647
VG 13	1.0500	1.088444	1.070184	1.099988	1.1	1.090123	1.098893
Ta 6-9	1.0780	1.01364	0.993708	0.996884	1.1	1.008815	1.044226
Ta 6-10	1.0690	1.045173	1.042592	0.949036	0.9	0.946162	0.904684
Ta 4-12	1.0320	1.063428	1.018614	1.031631	0.990567	0.975652	0.977235
Ta 28-27	1.0680	1.020301	0.991104	0.976953	0.989463	0.983985	0.979132
Qr 10	0	5	2.966956	4.374692	5	3.411287	4.844738
Qr 12	0	3.430701	0.713832	4.366721	1.5E-06	2.250819	4.864826
Qr 15	0	1.754133	1.657207	4.974559	5	2.335161	4.557783
Qr 17	0	4.858897	1.784874	0.865704	5	3.443132	4.902339
Qr 20	0	5	2.792935	2.802873	4.40039	2.022624	3.614843
Qr 21	0	5	1.804884	4.07292	5	4.225295	4.840288
Qr 23	0	5	1.079345	1.849487	2.71585	3.516276	3.594097
Qr 24	0	5	3.888447	4.716259	5	4.033772	4.583233
Qr 29	0	5	2.454247	2.050629	2.271475	4.504769	2.553763
PG 1	99.2400	51.36892	56.25298	51.43609	51.18571	52.70405	51.57972
PG 2	80	80	78.58037	79.97287	80	79.32674	79.6883
PG 5	50	50	49.96991	49.99684	50	49.90259	49.93927
PG 8	20	35	33.73529	34.99919	35	34.92388	34.9989
PG 11	20	30	28.5719	29.97878	30	29.87712	29.99568
PG 13	20	40	39.47651	39.89602	40	39.68273	39.9928
First TCSC installed Lines	-	10-17	9-11	28-27	6-28	15-23	28-27
First TCSC Compensation	-	-39.76%	-0.62%	-44.65%	-36.96%	-14.12%	-48.39%
Second TCSC installed Lines	-	6-28	12-13	6-7	10-20	16-17	4-12
Second TCSC Compensation	-	6.83%	-7.28%	-5.97%	-50.00%	-14.06%	45.30%
Third TCSC installed Lines	-	25-26	-	10-20	28-27	23-24	6-7
Third TCSC Compensation	-	-50.00%	-	-49.50%	-50.00%	-37.21%	47.00%
Losses (MW)	5.832400	2.969	3.187	2.880	2.821	3.017108	2.794672

Positive and negative indications represent an increase or decrease in the transmission line reactance connected with TCSC, respectively.

transmission lines (4-12) and (2-5) with compensation levels of 49.78% addition and 25% subtraction from the installed line reactance, respectively. The IDMO over the original case accomplished a 51.95% reduction in power losses.

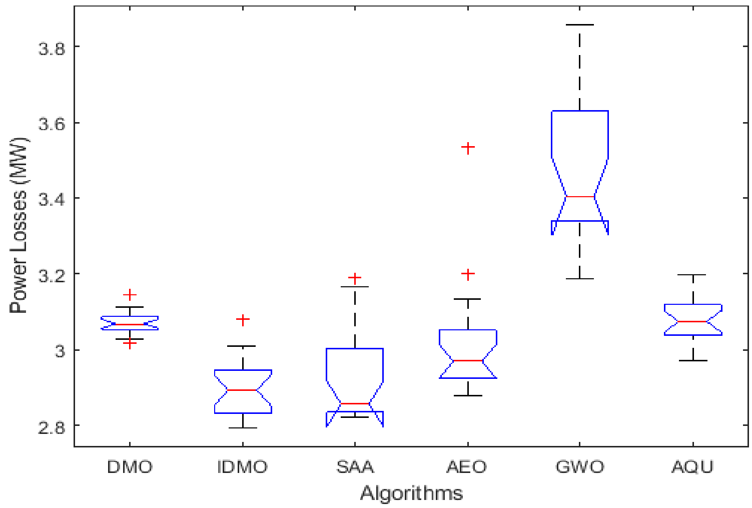

FIGURE 10. Box plot related to the outcomes of the compared algorithms for Case 3.

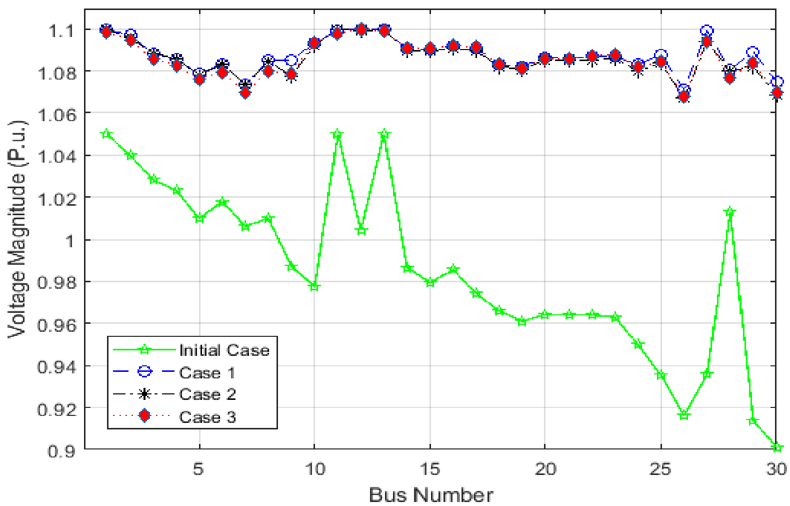

FIGURE 11. Voltages profile after candidate TCSC installment for cases 1-3 using the designed IDMO.

TABLE 11. Statistical outcomes of the obtained losses (MW) for Case 3.

	DMO	IDMO	SAA	AEO	GWO	AQU
Best	3.017	2.795	2.821	2.880	3.187	2.969
Mean	3.071	2.898	2.918	3.010	3.468	3.079
Worst	3.143	3.080	3.189	3.536	3.856	3.198
STD	0.029	0.073	0.123	0.150	0.173	0.066
Time*	0.690	0.710	0.542	0.975	0.766	0.999

Time indicates the average time per iteration measured in seconds.

In comparison to results achieved by the standard DMO, the proposed IDMO achieves a 7.46% reduction in power losses. The proposed IDMO achieves a 6.87% reduction when compared to the obtained results by the AQU. In addition, the proposed IDMO achieves a 15.14% reduction compared to GWO. Additionally, the proposed IDMO achieves a 2.3% reduction when compared to AEO and SAA.

Fig. 8 displays the box plot related to Case 2 to estimate the statistical indices of the applied techniques. Table 9 displays the associated statistical outcomes of the obtained Losses (MW) for this case. Using the mean acquired losses and the worst acquired losses as bases, the proposed IDMO extracts the lowest indices of the obtained objective values. Comparing the IDMO's findings to those produced by the DMO, SAA, AEO, GWO, and AQU, respectively, shows improved reductions of 6.21%, 2.22%, 3.84%, 17.95%, and 7.47% based on the mean acquired losses. When compared to the findings produced by the DMO, SAA, AEO, GWO, and AQU, respectively, the suggested IDMO discovers improved reductions of 2.75%, 4.24%, 5.61%, 27.42%, and 4.62% based on the worst acquired losses.

TABLE 12. Outcomes of the compared algorithms for TCSC device allocations regarding Cases 1-3.

		Case 1		Case 2		Case 3	
	Initial Scenario	DMO	IDMO	DMO	IDMO	DMO	IDMO
Vg_{1}	1.010	1.029156	1.055399	1.017788	1.04775	1.007932	1.051661
Vg_{2}	1.010	1.01216	1.048466	1.002	1.042348	0.992942	1.044435
Vg_{3}	1.010	1.009199	1.052619	1.008656	1.054655	0.998492	1.046605
Vg_{6}	1.010	1.015682	1.057393	1.006801	1.070256	1.015478	1.049904
Vg_{8}	1.010	1.028094	1.065556	1.016439	1.079823	1.031396	1.053022
Vg_{9}	1.010	0.999384	1.044359	0.996696	1.048386	1.000715	1.0309
Vg_{12}	1.010	0.999002	1.049063	1.012335	1.038555	1.001056	1.036724
$Tap_{4\text{-}18}$	0.970	1.052404	0.928202	1.047611	1.03564	1.042464	0.960822
$Tap_{4\text{-}18}$	0.978	0.963536	0.974739	1.074266	0.997582	0.964078	1.012136
$Tap_{21\text{-}20}$	1.043	0.948827	0.99604	0.93705	1.075473	1.038865	1.032366
$Tap_{24\text{-}25}$	1.000	1.005515	0.928102	1.021563	1.012975	1.002942	1.01449
$Tap_{24\text{-}25}$	1.000	0.971179	1.082998	0.989687	1.008818	1.0684	1.048149
$Tap_{24\text{-}26}$	1.043	0.991316	1.005914	1.017962	1.008848	1.017281	0.993082
$Tap_{7\text{-}29}$	0.967	0.980754	0.957808	1.026711	0.967861	0.993982	0.957576
$Tap_{34\text{-}32}$	0.975	0.982885	0.980212	1.005269	0.961879	1.024749	0.949418
$Tap_{11\text{-}41}$	0.955	1.038914	0.910106	0.932378	0.908157	0.961831	0.914396
$Tap_{15\text{-}45}$	0.955	0.943313	0.945486	0.968472	0.937494	0.925017	0.940501
$Tap_{14\text{-}46}$	0.900	0.994661	0.936625	0.967083	0.933566	0.910426	0.942134
$Tap_{10\text{-}51}$	0.930	1.001696	0.953009	0.9587	0.947167	0.966417	0.940568
$Tap_{13\text{-}49}$	0.895	0.928278	0.925885	0.942943	0.91396	0.909518	0.930535
$Tap_{11\text{-}43}$	0.958	0.981477	0.982129	1.024464	0.930207	0.956848	0.936254
$Tap_{40\text{-}56}$	0.958	1.027998	1.009618	1.003132	0.994886	0.980958	1.01481
$Tap_{39\text{-}57}$	0.980	0.991682	0.972984	0.982698	0.978169	0.973298	0.940079
$Tap_{9\text{-}55}$	0.940	1.007147	0.964339	1.061374	0.953957	1.004027	0.941957
Qc_{18}	10.000	15.31775	1.550864	29.52335	5.954505	14.91417	11.68338
Qc_{25}	5.900	19.72919	12.92438	17.42499	12.88076	19.84854	17.22348
Qc_{53}	6.300	18.96992	12.79661	10.10077	11.23059	14.50879	9.863362
Pg_{1}	478.635	177.3609	189.2655	200.5117	185.2979	205.5998	197.388
Pg_{2}	0.000	65.07995	5.407112	39.10329	4.581609	53.09737	13.94101
Pg_{3}	40.000	94.47558	134.5214	124.0211	136.656	110.1488	131.4228
Pg_{6}	0.000	77.06884	98.80492	53.46179	99.91842	47.34087	96.94933
Pg_{8}	450.000	365.432	323.0517	346.953	325.6818	360.6855	312.4387
Pg_{9}	0.000	84.73127	99.62949	96.75116	99.21885	81.42472	99.45746
Pg_{12}	310.000	399.954	409.9662	403.0061	409.3974	405.7088	408.949
First TCSC installed Lines	-	12-17	19-20	4-18	14-46	24-25	24-25
First TCSC Compensation	-	0.05%	9.68%	-27.89%	10.62%	0.02%	20.42%
Second TCSC installed Lines	-	-	-	13-15	10-51	6-7	21-22
Second TCSC Compensation	-	-	-	-13.79%	-6.39%	4.28%	-27.97%
Third TCSC installed Lines	-	-	-	-	-	22-23	13-49
Third TCSC Compensation	-	-	-	-	-	-44.30%	-44.55%
Losses (MW)	27.835	13.30243	9.846252	13.00813	9.951942	13.20578	9.746247

Positive and negative indications represent an increase or decrease in the transmission line reactance connected with TCSC, respectively.

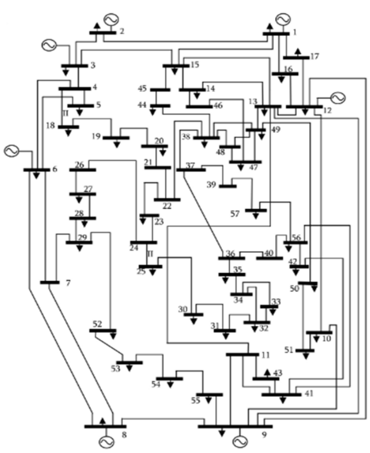

FIGURE 12. IEEE 57-bus power system [79].

3) CASE 3

In this case, the allocations of three TCSC devices are optimized to get the minimum power losses using the proposed IDMO and the other algorithms. Table 10 displays the control variables, and the related converging properties are shown in Fig. 9. The developed IDMO gets the lowest power losses of 2.795 MW. The locations of the three TCSC are the transmission lines (28-17), (4-12), and (6-7) with compensation level of 48.39% subtraction, 45.3% addition, and 47% addition, respectively.

Based on the best outcomes stated in Table 10, the proposed IDMO achieves 7.37%, 0.95%, 2.96%, 12.31%, and 5.87% reduction in power losses with comparing to the DMO, SAA, AEO, GWO and AQU, respectively. Fig. 10 displays the box plot related to the outcomes of the compared algorithms for Case 3. Table 11 displays the associated statistical outcomes of the obtained Losses (MW) for this case. Based on the mean acquired losses, the proposed IDMO accomplishes 5.65%, 0.68%, 3.72%, 16.44%, and 5.88% reduction in power losses in compared to the obtained results by the DMO, SAA, AEO, GWO and AQU, respectively. Based on the worst acquired losses, the proposed IDMO finds 1.99%, 3.43%, 12.90%, 20.11% and 3.69% reduction when

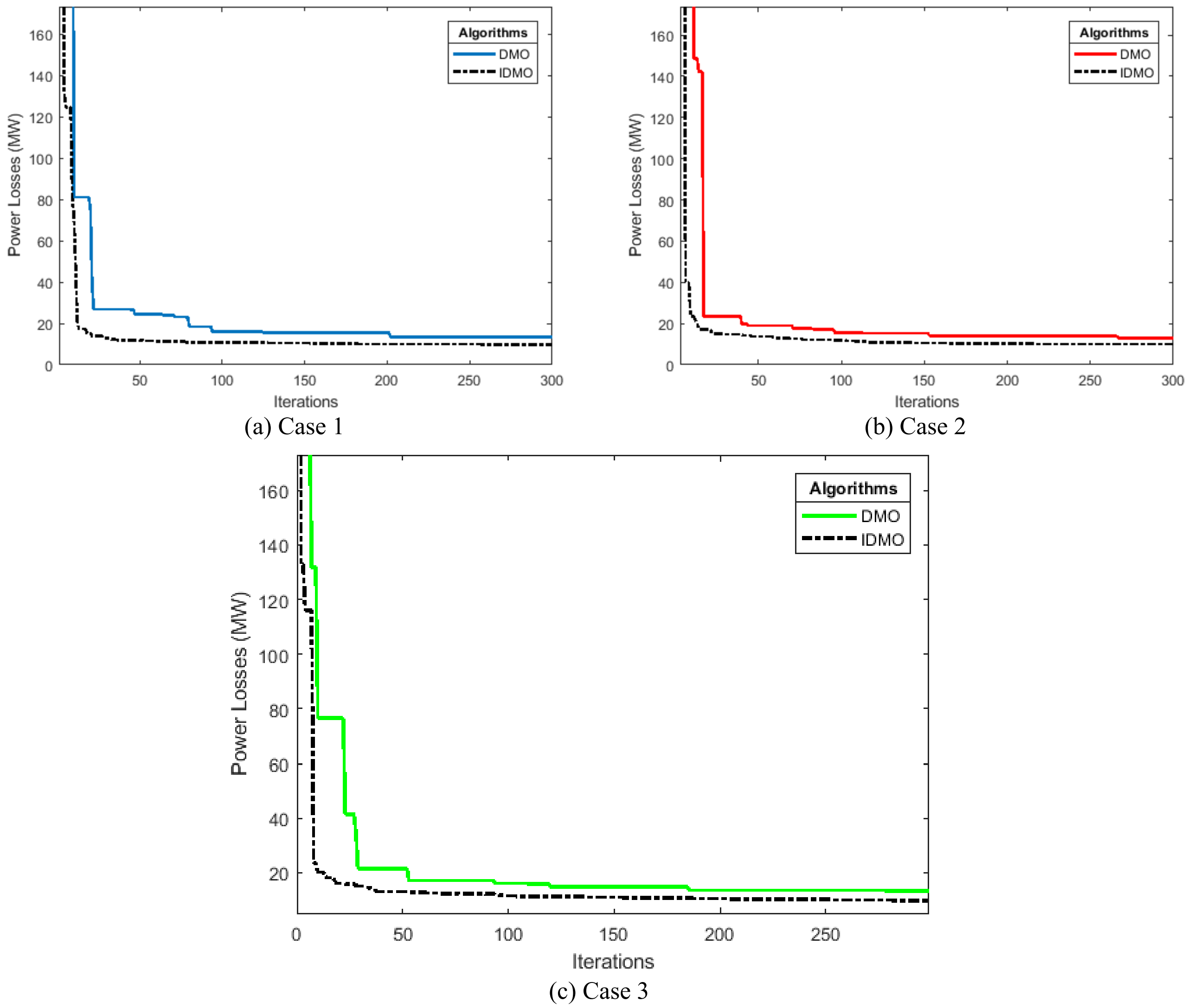

FIGURE 13. Implemented algorithms' convergence curves regarding Cases 1-3.

compared to the obtained results by the DMO, SAA, AEO, GWO and AQU, respectively.

4) VOLTAGE PROFILE-BASED TCSC INSTALLATIONS FOR THE IEEE 30-BUS SYSTEM

Based on the utilized TCSC using the proposed IDMO, the voltages profiles in the previous three cases are represented in Fig. 11 compared to the initial case.

Grid buses have improved significantly for the three situations examined, as has been observed. The biggest voltage increase is on the last grid bus (No. 30), which goes from 0.9012 per unit (p.u.) to 1.075, 1.0686 and 1.0699 p.u. with improvements of 16.17%, 15.67% and 15.77% for the Cases 1, 2, and 3, respectively.

C. APPLICATIONS FOR TCSC ALLOCATIONS IN IEEE STANDARD 57-BUS TRANSMISSION NETWORK

The standard IEEE 57-bus transmission network, illustrated in Fig. 12, is utilized in this section. This system consists of 57 nodes, 80 lines, 17 on-load tap changing transformers, 7 generators, and three capacitive sources on buses. The system data is extracted from [78]. The three cases studied are investigated considering one, two and three TCSC devices to reduce the power losses. The IDMO and DMO are applied where Table 12 tabulates their obtained control variables. As shown, the proposed IDMO shows higher reduced power losses of 9.846, 9.952 and 9.746 MW compared to 13.302, 13.008 and 13.206 MW for the cases 1-3, respectively. Otherwise, the converging properties are depicted in Fig. 13. The proposed IDMO shows better searching capability over the standard DMO in finding and developing the best individual through the iterations.

Moreover, Fig. 14 displays the box plot related to the outcomes of the compared algorithms for all considered cases. As demonstrated, the suggested IDMO performs best by gaining the fewest indices among the acquired objective values. From this figure, it can be concluded the following:

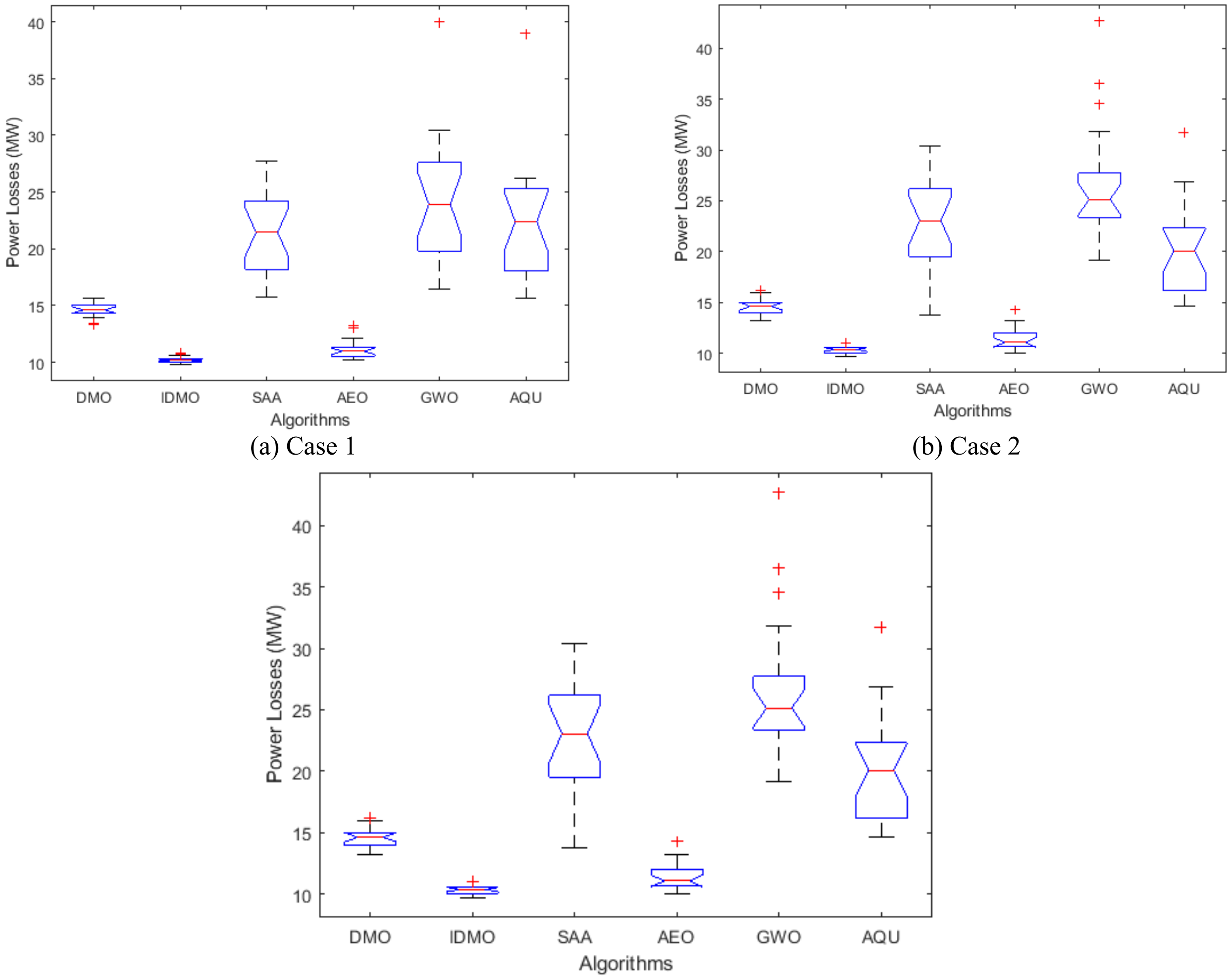

(a) Case 1 (b) Case 2

(c) Case 3

FIGURE 14. Box plot related to the outcomes of IDMO, DMO, AEO, SAA, AQU, and GWO for Cases 1-3.

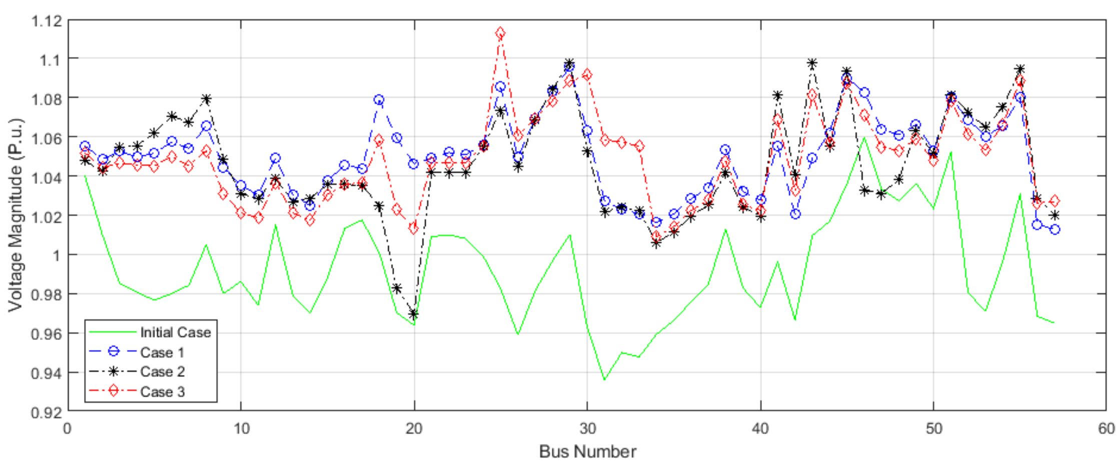

FIGURE 15. Voltages profile after candidate TCSC installment for cases 1-3 using the designed IDMO for the second system.

- For the first case, based on the mean acquired losses, the proposed IDMO finds the least losses of 10.215 MW while DMO, SAA, AEO, GWO and AQU obtain losses of 14.611, 21.300, 11.138, 24.544 and 22.346, respectively. Therefore, the proposed IDMO achieves improvement reduction 30.08%, 52.04%, 8.28%, 58.38% and 54.28% respectively, compared to the obtained results by the DMO, SAA, AEO, GWO and AQU.

- For the second case, based on the mean acquired losses, the proposed IDMO finds the least losses of 11.124 MW while DMO, SAA, AEO, GWO and AQU obtain losses of 15.613, 25.016, 15.288, 32.709 and 30.916, respectively. Therefore, the proposed IDMO achieves improvement reduction 28.75%, 55.53%, 27.23%, 65.99% and 64.02%, respectively, compared to the obtained results by the DMO, SAA, AEO, GWO and AQU.
- For the third case, based on the mean acquired losses, the proposed IDMO finds the least losses of 10.33 MW while DMO, SAA, AEO, GWO and AQU obtain losses of 14.541, 22.554, 11.406, 26.476 and 20.072, respectively. Therefore, the proposed IDMO achieves improvement reduction 28.96%, 54.20%, 9.44%, 60.99% and 48.54%, respectively, compared to the obtained results by the DMO, SAA, AEO, GWO and AQU.

Based on the candidate TCSC installment using the designed IDMO in the previous cases, the voltages profile over all the system buses are depicted in Fig. 15 compared to the initial case.

As can be shown, grid buses have significantly improved in each of the scenarios examined. The largest voltage profile rise is seen on the last grid bus (No. 31), which increased from 0.9359 p.u. to 1.027, 1.022, and 1.058 p.u. with improvements of 8.87%, 8.42%, and 11.54% for Cases 1-3, respectively.

V. CONCLUSION

This paper provides a revolutionary IDMO incorporating an ADLP for dealing with a variety of mathematical benchmark functions and technical difficulties. The creatively proposed technique has an improved learning strategy to improve searching features, and portion of its update operation is driven by the updated alpha. Firstly, the suggested IDMO is opposed to the conventional DMO and assessed using CEC 2017 single objective criteria. The designed IDMO achieves the least average rank of 2.517 achieving the superior outcomes by obtaining the first rank. It shows improvement reduction of 25.79%, 42.21%, 46.99%, 51.71%, 52.20%, 56.75%, 62.89%, 68.94% and 71.22% in comparison to EO, SMA, ESMA, GTO, DMO, AEO, RKO, SAA and AQU, respectively. Furthermore, the application is conducted for optimal allocation of TCSC devices in transmission power systems considering two different IEEE power systems of 30 and 57 buses and considering different number of TCSC devices. For all applications, the suggested IDMO outperforms the DMO, SAA, AEO, GWO, and AQU by accumulating the fewest indexes of the acquired values for objective. Additionally, the overall grid buses have advanced significantly in all scenarios examined for the two IEEE systems.

REFERENCES

[1] J. Singh, N. K. Yadav, and S. K. Gupta, "Enhancement of available transfer capability using TCSC with hybridized model: Combining lion and moth flame algorithms," *Concurrency Comput., Pract. Exper.*, vol. 34, no. 21, Sep. 2022, doi: 10.1002/cpe.7052.

[2] A. K. Bhullar, R. Kaur, and S. Sondhi, "Modified neural network algorithm based robust design of AVR system using the Kharitonov theorem," *Int. J. Intell. Syst.*, vol. 37, no. 2, pp. 1339–1370, Feb. 2022, doi: 10.1002/int.22672.

[3] G. Xiong, X. Yuan, A. W. Mohamed, and J. Zhang, "Fault section diagnosis of power systems with logical operation binary gaining-sharing knowledge-based algorithm," *Int. J. Intell. Syst.*, vol. 37, no. 2, pp. 1057–1080, Feb. 2022, doi: 10.1002/int.22659.

[4] S. Murali and R. Shankar, "Exploration of novel optimal fuzzy-based controller for enhancement of frequency regulation of deregulated hybrid power system with modified HVDC tie-line," *Int. J. Intell. Syst.*, vol. 37, no. 7, pp. 4163–4189, Jul. 2022, doi: 10.1002/int.22715.

[5] S. Dash, K. R. Subhashini, and J. Satapathy, "Efficient utilization of power system network through optimal location of FACTS devices using a proposed hybrid meta-heuristic ant lion-moth flame-salp swarm optimization algorithm," *Int. Trans. Electr. Energy Syst.*, vol. 30, no. 7, Jul. 2020, doi: 10.1002/2050-7038.12402.

[6] R. Devarapalli, B. Bhattacharyya, and N. K. Sinha, "An intelligent EGWO-SCA-CS algorithm for PSS parameter tuning under system uncertainties," *Int. J. Intell. Syst.*, vol. 35, no. 10, pp. 1520–1569, Oct. 2020, doi: 10.1002/int.22263.

[7] R. M. Mathur and R. K. Varma, *Thyristor-Based Facts Controllers for Electrical Transmission Systems*. Wiley, 2002.

[8] C. Rehtanz, *Flexible AC Transmission Systems: Modelling and Control* (Power Systems), 2 ed. Berlin, Germany: Springer, 2006. [Online]. Available: https://doi.org/10.1007/978-3-642-28241-6

[9] J. Morsali, K. Zare, and M. T. Hagh, "Performance comparison of TCSC with TCPS and SSSC controllers in AGC of realistic interconnected multi-source power system," *Ain Shams Eng. J.*, vol. 7, no. 1, pp. 143–158, Mar. 2016, doi: 10.1016/j.asej.2015.11.012.

[10] A. M. Shaheen, R. A. El-Sehiemy, and S. M. Farrag, "Optimal reactive power dispatch using backtracking search algorithm," *Austral. J. Electr. Electron. Eng.*, vol. 13, no. 3, pp. 200–210, Jul. 2016, doi: 10.1080/1448837X.2017.1325134.

[11] R. A. El Sehiemy, A. A. A. El Ela, and A. Shaheen, "A multi-objective fuzzy-based procedure for reactive power-based preventive emergency strategy," *Int. J. Eng. Res. Afr.*, vol. 13, pp. 91–102, Dec. 2014, doi: 10.4028/www.scientific.net/JERA.13.91.

[12] A. E. Chaib, H. R. E. H. Bouchekara, R. Mehasni, and M. A. Abido, "Optimal power flow with emission and non-smooth cost functions using backtracking search optimization algorithm," *Int. J. Electr. Power Energy Syst.*, vol. 81, pp. 64–77, Oct. 2016, doi: 10.1016/j.ijepes.2016.02.004.

[13] S. S. Reddy and P. R. Bijwe, "Efficiency improvements in meta-heuristic algorithms to solve the optimal power flow problem," *Int. J. Emerg. Electr. Power Syst.*, vol. 17, no. 6, pp. 631–647, Dec. 2016, doi: 10.1515/ijeeps-2015-0216.

[14] H. R. E.-H. Bouchekara, M. A. Abido, and A. E. Chaib, "Optimal power flow using an improved electromagnetism-like mechanism method," *Electr. Power Compon. Syst.*, vol. 44, no. 4, pp. 434–449, Feb. 2016, doi: 10.1080/15325008.2015.1115919.

[15] I. Ziane, F. Benhamida, and A. Graa, "Simulated annealing algorithm for combined economic and emission power dispatch using max/max price penalty factor," *Neural Comput. Appl.*, vol. 28, no. 1, pp. 197–205, Dec. 2017, doi: 10.1007/s00521-016-2335-3.

[16] M. Ghasemi, S. Ghavidel, M. Gitizadeh, and E. Akbari, "An improved teaching-learning-based optimization algorithm using Lévy mutation strategy for non-smooth optimal power flow," *Int. J. Electr. Power Energy Syst.*, vol. 65, pp. 375–384, Feb. 2015, doi: 10.1016/j.ijepes.2014.10.027.

[17] H. R. E. H. Bouchekara, A. E. Chaib, and M. A. Abido, "Optimal power flow using GA with a new multi-parent crossover considering: Prohibited zones, valve-point effect, multi-fuels and emission," *Electr. Eng.*, vol. 100, no. 1, pp. 151–165, Mar. 2018, doi: 10.1007/s00202-016-0488-9.

[18] A. A. El-Fergany and H. M. Hasanien, "Single and multi-objective optimal power flow using grey wolf optimizer and differential evolution algorithms," *Electr. Power Compon. Syst.*, vol. 43, no. 13, pp. 1548–1559, Aug. 2015, doi: 10.1080/15325008.2015.1041625.

[19] B. Bentouati, M. S. Javaid, H. R. E. H. Bouchekara, and A. A. El-Fergany, "Optimizing performance attributes of electric power systems using chaotic salp swarm optimizer," *Int. J. Manage. Sci. Eng. Manage.*, vol. 15, no. 3, pp. 165–175, Jul. 2020, doi: 10.1080/17509653.2019.1677197.

[20] G. Moustafa, M. Elshahed, A. R. Ginidi, A. M. Shaheen, and H. S. E. Mansour, "A gradient-based optimizer with a crossover operator for distribution static VAR compensator (D-SVC) sizing and placement in electrical systems," *Mathematics*, vol. 11, no. 5, p. 1077, Feb. 2023, doi: 10.3390/math11051077.

[21] A. R. Kumar and L. Premalatha, "Optimal power flow for a deregulated power system using adaptive real coded biogeography-based optimization," *Int. J. Electr. Power Energy Syst.*, vol. 73, pp. 393–399, Dec. 2015, doi: 10.1016/j.ijepes.2015.05.011.

[22] M. Basu, "Modified particle swarm optimization for nonconvex economic dispatch problems," *Int. J. Electr. Power Energy Syst.*, vol. 69, pp. 304–312, Jul. 2015, doi: 10.1016/j.ijepes.2015.01.015.

[23] S. Khalilpourazari and S. Khalilpourazary, "An efficient hybrid algorithm based on water cycle and moth-flame optimization algorithms for solving numerical and constrained engineering optimization problems," *Soft Comput.*, vol. 23, no. 5, pp. 1699–1722, Mar. 2019, doi: 10.1007/s00500-017-2894-y.

[24] A. Dabba, A. Tari, and S. Meftali, "Hybridization of moth flame optimization algorithm and quantum computing for gene selection in microarray data," *J. Ambient Intell. Humanized Comput.*, vol. 12, no. 2, pp. 2731–2750, Feb. 2021, doi: 10.1007/s12652-020-02434-9.

[25] M. Bouaraki and A. Recioui, "Optimal placement of power factor correction capacitors in power systems using teaching learning based optimization," *Algerian J. Signals Syst.*, vol. 2, no. 2, pp. 102–109, Jun. 2017, doi: 10.51485/ajss.v2i2.37.

[26] E. E. Elattar and S. K. ElSayed, "Modified Jaya algorithm for optimal power flow incorporating renewable energy sources considering the cost, emission, power loss and voltage profile improvement," *Energy*, vol. 178, pp. 598–609, Jul. 2019, doi: 10.1016/j.energy.2019.04.159.

[27] T. T. Nguyen, "A high performance social spider optimization algorithm for optimal power flow solution with single objective optimization," *Energy*, vol. 171, pp. 218–240, Mar. 2019, doi: 10.1016/j.energy.2019.01.021.

[28] M. Kaur and N. Narang, "An integrated optimization technique for optimal power flow solution," *Soft Comput.*, vol. 24, no. 14, pp. 10865–10882, Jul. 2020, doi: 10.1007/s00500-019-04590-3.

[29] A. Shaheen, A. Ginidi, R. El-Sehiemy, A. Elsayed, E. Elattar, and H. T. Dorrah, "Developed gorilla troops technique for optimal power flow problem in electrical power systems," *Mathematics*, vol. 10, no. 10, p. 1636, May 2022, doi: 10.3390/MATH10101636.

[30] A. Ginidi, E. Elattar, A. Shaheen, A. Elsayed, R. El-Sehiemy, and H. Dorrah, "Optimal power flow incorporating Thyristor-controlled series capacitors using the gorilla troops algorithm," *Int. Trans. Electr. Energy Syst.*, vol. 2022, pp. 1–23, Aug. 2022, doi: 10.1155/2022/9448199.

[31] A. M. Shaheen, R. A. El-Sehiemy, E. E. Elattar, and A. S. Abd-Elrazek, "A modified crow search optimizer for solving non-linear OPF problem with emissions," *IEEE Access*, vol. 9, pp. 43107–43120, 2021, doi: 10.1109/ACCESS.2021.3060710.

[32] V. S. Rao, M. Ravindra, A. S. Veerendra, R. S. Rao, A. Ramesh, and K. M. K. Reddy, "Sensitivity based allocation of FACTS devices in a transmission system considering differential analysis," in *Proc. Int. Conf. Artif. Intell. Techn. Elect. Eng. Syst. (AITEES)*, 2023, pp. 48–60.

[33] N. K. Yadav, "Optimizing TCSC configuration via genetic algorithm for ATC enhancement," *Multimedia Tools Appl.*, vol. 82, no. 25, pp. 38715–38741, Oct. 2023, doi: 10.1007/s11042-023-15043-3.

[34] G. Moustafa, M. A. Tolba, A. M. El-Rifaie, A. Ginidi, A. M. Shaheen, and S. Abid, "A subtraction-average-based optimizer for solving engineering problems with applications on TCSC allocation in power systems," *Biomimetics*, vol. 8, no. 4, p. 332, Jul. 2023, doi: 10.3390/biomimetics8040332.

[35] W. Liu, X. Yang, T. Zhang, and A. Abu-Siada, "Multi-objective optimal allocation of TCSC for power systems with wind power considering load randomness," *J. Electr. Eng. Technol.*, vol. 18, no. 2, pp. 765–777, Sep. 2022, doi: 10.1007/s42835-022-01233-w.

[36] J. O. Agushaka, A. E. Ezugwu, and L. Abualigah, "Dwarf mongoose optimization algorithm," *Comput. Methods Appl. Mech. Eng.*, vol. 391, Mar. 2022, Art. no. 114570, doi: 10.1016/j.cma.2022.114570.

[37] O. A. Akinola, A. E. Ezugwu, O. N. Oyelade, and J. O. Agushaka, "A hybrid binary dwarf mongoose optimization algorithm with simulated annealing for feature selection on high dimensional multi-class datasets," *Sci. Rep.*, vol. 12, no. 1, Sep. 2022, doi: 10.1038/s41598-022-18993-0.

[38] B. Singh, S. K. Bishnoi, and M. Sharma, "Frequency regulation scheme for PV integrated power system using energy storage device," in *Proc. Int. Conf. Intell. Controller Comput. Smart Power (ICICCSP)*, Jul. 2022, pp. 1–7, doi: 10.1109/ICICCSP53532.2022.9862387.

[39] A. M. Sadoun, I. R. Najjar, G. S. Alsoruji, A. Wagih, and M. A. Elaziz, "Utilizing a long short-term memory algorithm modified by dwarf mongoose optimization to predict thermal expansion of cu-Al_2O_3 nanocomposites," *Mathematics*, vol. 10, no. 7, p. 1050, Mar. 2022, doi: 10.3390/math10071050.

[40] A. Abirami and R. Kavitha, "An efficient early detection of diabetic retinopathy using dwarf mongoose optimization based deep belief network," *Concurrency Comput., Pract. Exper.*, vol. 34, no. 28, Dec. 2022, doi: 10.1002/cpe.7364.

[41] M. A. Elaziz, A. A. Ewees, M. A. A. Al-qaness, S. Alshathri, and R. A. Ibrahim, "Feature selection for high dimensional datasets based on quantum-based dwarf mongoose optimization," *Mathematics*, vol. 10, no. 23, p. 4565, Dec. 2022, doi: 10.3390/math10234565.

[42] S. Balasubramaniam, K. S. Kumar, V. Kavitha, A. Prasanth, and T. A. Sivakumar, "Feature selection and dwarf mongoose optimization enabled deep learning for heart disease detection," *Comput. Intell. Neurosci.*, vol. 2022, pp. 1–11, Dec. 2022, doi: 10.1155/2022/2819378.

[43] K. Mehmood, N. I. Chaudhary, Z. A. Khan, K. M. Cheema, M. A. Z. Raja, A. H. Milyani, and A. A. Azhari, "Dwarf mongoose optimization metaheuristics for autoregressive exogenous model identification," *Mathematics*, vol. 10, no. 20, p. 3821, Oct. 2022, doi: 10.3390/math10203821.

[44] B. K. Dora, S. Bhat, S. Halder, and I. Srivastava, "A solution to the techno-economic generation expansion planning using enhanced dwarf mongoose optimization algorithm," in *Proc. IEEE Bombay Sect. Signature Conf. (IBSSC)*, Dec. 2022, pp. 1–6, doi: 10.1109/IBSSC56953.2022.10037536.

[45] F. Aldosari, L. Abualigah, and K. H. Almotairi, "A normal distributed dwarf mongoose optimization algorithm for global optimization and data clustering applications," *Symmetry*, vol. 14, no. 5, p. 1021, May 2022, doi: 10.3390/sym14051021.

[46] L. Abualigah, D. Oliva, H. Jia, F. Gul, N. Khodadadi, A. G. Hussien, M. A. Shinwan, A. E. Ezugwu, B. Abuhaija, and R. A. Zitar, "Improved Prairie dog optimization algorithm by dwarf mongoose optimization algorithm for optimization problems," *Multimedia Tools Appl.*, Sep. 2023, doi: 10.1007/s11042-023-16890-w.

[47] J. O. Agushaka, A. E. Ezugwu, O. N. Olaide, O. Akinola, R. A. Zitar, and L. Abualigah, "Improved dwarf mongoose optimization for constrained engineering design problems," *J. Bionic Eng.*, vol. 20, no. 3, pp. 1263–1295, May 2023, doi: 10.1007/s42235-022-00316-8.

[48] I. Al-Shourbaji, P. Kachare, S. Fadlelseed, A. Jabbari, A. G. Hussien, F. Al-Saqqar, L. Abualigah, and A. Alameen, "Artificial ecosystem-based optimization with dwarf mongoose optimization for feature selection and global optimization problems," *Int. J. Comput. Intell. Syst.*, vol. 16, no. 1, Jun. 2023, doi: 10.1007/s44196-023-00279-6.

[49] *An Update on Power Quality*, D. Lu, Ed. InTech, 2013, doi: 10.5772/51135.

[50] C. Gupta, "Book review: FACTS: Modelling and simulation in power networks," *Int. J. Electr. Eng. Educ.*, vol. 42, no. 2, pp. 209–210, Apr. 2005, doi: 10.7227/ijeee.42.2.8.

[51] K. K. Sen and M. L. Sen, *Introduction to FACTS Controllers: Theory, Modeling, and Applications*. Wiley, Sep. 2009.

[52] W. S. Sakr, R. A. El-Sehiemy, and A. M. Azmy, "Optimal allocation of TCSCs by adaptive DE algorithm," *IET Gener., Transmiss. Distribution*, vol. 10, no. 15, pp. 3844–3854, Nov. 2016, doi: 10.1049/iet-gtd.2016.0362.

[53] M. B. Shafik, H. Chen, G. I. Rashed, and R. A. El-Sehiemy, "Adaptive multi objective parallel seeker optimization algorithm for incorporating TCSC devices into optimal power flow framework," *IEEE Access*, vol. 7, pp. 36934–36947, 2019, doi: 10.1109/ACCESS.2019.2905266.

[54] S. Sarhan, A. Shaheen, R. El-Sehiemy, and M. Gafar, "Optimal multi-dimension operation in power systems by an improved artificial hummingbird optimizer," in *Human-Centric Computing and Information Sciences*, vol. 13. Seoul, South Korea: Korea Information Processing Soc, 2023, Art. no. 13, doi: https://doi.org/10.22967/HCIS.2023.13.013.

[55] Y. Shen, Z. Liang, H. Kang, X. Sun, and Q. Chen, "A modified jSO algorithm for solving constrained engineering problems," *Symmetry*, vol. 13, no. 1, p. 63, Dec. 2020, doi: 10.3390/sym13010063.

[56] W. Zhao, L. Wang, and Z. Zhang, "Artificial ecosystem-based optimization: A novel nature-inspired meta-heuristic algorithm," *Neural Comput. Appl.*, vol. 32, no. 13, pp. 9383–9425, Jul. 2020, doi: 10.1007/s00521-019-04452-x.

[57] L. Abualigah, D. Yousri, M. A. Elaziz, A. A. Ewees, M. A. A. Al-qaness, and A. H. Gandomi, "Aquila optimizer: A novel meta-heuristic optimization algorithm," *Comput. Ind. Eng.*, vol. 157, Jul. 2021, Art. no. 107250, doi: 10.1016/j.cie.2021.107250.

[58] A. Faramarzi, M. Heidarinejad, B. Stephens, and S. Mirjalili, "Equilibrium optimizer: A novel optimization algorithm," *Knowl.-Based Syst.*, vol. 191, Mar. 2020, Art. no. 105190, doi: 10.1016/j.knosys.2019.105190.

[59] S. Sarhan, A. M. Shaheen, R. A. El-Sehiemy, and M. Gafar, "An enhanced slime mould optimizer that uses chaotic behavior and an elitist group for solving engineering problems," *Mathematics*, vol. 10, no. 12, p. 1991, Jun. 2022, doi: 10.3390/math10121991.

[60] B. Abdollahzadeh, F. S. Gharehchopogh, and S. Mirjalili, "Artificial gorilla troops optimizer: A new nature-inspired metaheuristic algorithm for global optimization problems," *Int. J. Intell. Syst.*, vol. 36, no. 10, pp. 5887–5958, Jul. 2021, doi: 10.1002/INT.22535.

[61] J. Raeisi-Gahruei and Z. Beheshti, "The electricity consumption prediction using hybrid red kite optimization algorithm with multi-layer perceptron neural network," *J. Intell. Procedures Elect. Technol.*, vol. 15, no. 60, 2022.

[62] P. Trojovský and M. Dehghani, "Subtraction-average-based optimizer: A new swarm-inspired metaheuristic algorithm for solving optimization problems," *Biomimetics*, vol. 8, no. 2, p. 149, Apr. 2023, doi: 10.3390/biomimetics8020149.

[63] S. Li, H. Chen, M. Wang, A. A. Heidari, and S. Mirjalili, "Slime mould algorithm: A new method for stochastic optimization," *Future Gener. Comput. Syst.*, vol. 111, pp. 300–323, Oct. 2020, doi: 10.1016/j.future.2020.03.055.

[64] A. Shaheen, A. Elsayed, A. Ginidi, R. El-Sehiemy, and E. Elattar, "Reconfiguration of electrical distribution network-based DG and capacitors allocations using artificial ecosystem optimizer: Practical case study," *Alexandria Eng. J.*, vol. 61, no. 8, pp. 6105–6118, Aug. 2022, doi: 10.1016/J.AEJ.2021.11.035.

[65] N. Van Thieu, S. Deb Barma, T. Van Lam, O. Kisi, and A. Mahesha, "Groundwater level modeling using augmented artificial ecosystem optimization," *J. Hydrol.*, vol. 617, Feb. 2023, Art. no. 129034, doi: 10.1016/J.JHYDROL.2022.129034.

[66] A. Mahdy, R. El-Sehiemy, A. Shaheen, A. Ginidi, and Z. M. S. Elbarbary, "An improved artificial ecosystem algorithm for economic dispatch with combined heat and power units," *Appl. Sci.*, vol. 12, no. 22, p. 11773, Nov. 2022, doi: 10.3390/app122211773.

[67] Y. Niu, X. Yan, Y. Wang, and Y. Niu, "Three-dimensional UCAV path planning using a novel modified artificial ecosystem optimizer," *Expert Syst. Appl.*, vol. 217, May 2023, Art. no. 119499, doi: 10.1016/J.ESWA.2022.119499.

[68] A. A. A. El-Ela, R. A. El-Sehiemy, A. M. Shaheen, and A. S. Shalaby, "Aquila optimization algorithm for wind energy potential assessment relying on Weibull parameters estimation," *Wind*, vol. 2, no. 4, pp. 617–635, Sep. 2022, doi: 10.3390/wind2040033.

[69] M. H. Ali, A. T. Salawudeen, S. Kamel, H. B. Salau, M. Habil, and M. Shouran, "Single- and multi-objective modified Aquila optimizer for optimal multiple renewable energy resources in distribution network," *Mathematics*, vol. 10, no. 12, p. 2129, Jun. 2022, doi: 10.3390/math10122129.

[70] A. A. A. El-Ela, R. A. El-Sehiemy, A. M. Shaheen, W. A. Wahbi, and M. T. Mouwafi, "A multi-objective equilibrium optimization for optimal allocation of batteries in distribution systems with lifetime maximization," *J. Energy Storage*, vol. 55, Nov. 2022, Art. no. 105795.

[71] A. M. Shaheen, M. A. Hamida, R. A. El-Sehiemy, and E. E. Elattar, "Optimal parameter identification of linear and non-linear models for Li-ion battery cells," *Energy Rep.*, vol. 7, pp. 7170–7185, Nov. 2021, doi: 10.1016/j.egyr.2021.10.086.

[72] A. A. A. El-Ela, S. M. Allam, A. M. Shaheen, and N. A. Nagem, "Optimal allocation of biomass distributed generation in distribution systems using equilibrium algorithm," *Int. Trans. Electr. Energy Syst.*, vol. 31, no. 2, Feb. 2021, doi: 10.1002/2050-7038.12727.

[73] S. Abid, A. M. El-Rifaie, M. Elshahed, A. R. Ginidi, A. M. Shaheen, G. Moustafa, and M. A. Tolba, "Development of slime mold optimizer with application for tuning cascaded PD-PI controller to enhance frequency stability in power systems," *Mathematics*, vol. 11, no. 8, p. 1796, Apr. 2023, doi: 10.3390/math11081796.

[74] A. Shaheen, R. El-Sehiemy, A. El-Fergany, and A. Ginidi, "Fuel-cell parameter estimation based on improved gorilla troops technique," *Sci. Rep.*, vol. 13, no. 1, p. 8685, May 2023, doi: 10.1038/s41598-023-35581-y.

[75] A. M. Shaheen, R. A. El-Sehiemy, M. M. Alharthi, S. S. M. Ghoneim, and A. R. Ginidi, "Multi-objective jellyfish search optimizer for efficient power system operation based on multi-dimensional OPF framework," *Energy*, vol. 237, Dec. 2021, Art. no. 121478, doi: 10.1016/J.ENERGY.2021.121478.

[76] M. Ghasemi, M. Taghizadeh, S. Ghavidel, J. Aghaei, and A. Abbasian, "Solving optimal reactive power dispatch problem using a novel teaching-learning-based optimization algorithm," *Eng. Appl. Artif. Intell.*, vol. 39, pp. 100–108, Mar. 2015, doi: 10.1016/j.engappai.2014.12.001.

[77] S. Sarhan, A. Shaheen, R. El-Sehiemy, and M. Gafar, "An augmented social network search algorithm for optimal reactive power dispatch problem," *Mathematics*, vol. 11, no. 5, p. 1236, Mar. 2023, doi: 10.3390/math11051236.

[78] A. Shabanpour-Haghighi, A. R. Seifi, and T. Niknam, "A modified teaching-learning based optimization for multi-objective optimal power flow problem," *Energy Convers. Manage.*, vol. 77, pp. 597–607, Jan. 2014, doi: 10.1016/j.enconman.2013.09.028.

[79] A. M. Shaheen, R. A. El-Sehiemy, A. M. Elsayed, and E. E. Elattar, "Multi-objective manta ray foraging algorithm for efficient operation of hybrid AC/DC power grids with emission minimisation," *IET Gener., Transmiss. Distrib.*, vol. 15, no. 8, pp. 1314–1336, Apr. 2021, doi: 10.1049/gtd2.12104.

HASHIM ALNAMI received the bachelor's degree in electrical engineering from Jazan University, Jazan, Saudi Arabia, in 2013, the master's degree in electrical engineering specialist in electrical power systems from Southern Illinois University, IL, USA, in 2018, and the Ph.D. degree in electrical engineering specialist in electrical power systems from Wichita state University, KS, USA, in 2021. He was a Power Engineer with Saudi Aramco Company, Dhahran, Saudi Arabia, from 2013 to 2014. Since 2021, he has been an Assistant Professor with the Electrical Engineering Department, Jazan University. His research interests include power system distribution, power generation, power system analysis, renewable energy sources, and power control.

ALI M. EL-RIFAIE (Senior Member, IEEE) received the B.Sc. degree in electrical power and machines, the M.Sc. degree in electrical power system engineering, and the Ph.D. degree in power system protection from Helwan University, Egypt, in 1998, 2005, and 2011, respectively. From 2000 to 2004, he was a Demonstrator with the Electrical Power and Machines Department, Faculty of Engineering and Technology, Helwan University. From 2005 to 2010, he was a Research Assistant with the Egyptian National Institute for Standards (NIS), where he was also a Researcher with the High Voltage Metrology Laboratory, from 2010 to 2015. He was also the Proficiency Test Manager and held a laboratory technical position. Since September 2015, he has been with the American University of the Middle East, Kuwait. He is currently an Associate Professor with the Electrical Engineering Department. He is the author of one book and several peer-reviewed conferences and journal articles in power system protection, electrical metrology, smart grids, and renewable energy. He is an active member in several peer-reviewed journals and conferences technical committees. He received twice the Best Paper from EEEIC, London.

GHAREEB MOUSTAFA received the bachelor's and master's degrees in electrical engineering from Suez Canal University, Egypt, in 1998 and 2003, respectively, and the joint Ph.D. degree in electrical engineering with cooperation channel system from Suez Canal University, Egypt, and Dresden Technical University—TUD, Germany, in 2010. From 1998 to 2003, he was a Research and Teaching Assistant with the Electrical and Computer Engineering Department, Faculty of Engineering, Suez Canal University, as an Assistant Lecturer, from 2003 to 2007. From 2007 to 2009, he was a Researcher and a Visiting Ph.D. Student with the Institute of High Voltage and Current, TUD. From 2010 to 2013, he was a Lecturer with the Electrical Engineering Department, Faculty of Engineering, Suez Canal University. Since 2013, he has been an Assistant Professor with the Electrical Engineering Department, Faculty of Engineering, Jazan University, Jazan, Saudi Arabia. His research interests include high voltage and high current, electric connector, power quality, and recently power system optimization.

SULTAN H. HAKMI received the bachelor's degree in electrical engineering from the King Fahd University of Petroleum & Minerals, Saudi Arabia, in 2013, and the master's and Ph.D. degrees in electrical engineering specialist in electrical power systems from Wichita State University, KS, USA, in 2017 and 2021, respectively. He was a Teaching Assistant with the Electrical Engineering Department, Jazan University, Jazan, Saudi Arabia, from 2013 to 2014. From 2016 to 2021, he was a Research Assistant, while he was a student with the Electrical Engineering Department, Wichita State University, KS, USA. Since 2021, he has been an Assistant Professor with the Electrical Engineering Department, Jazan University. His research interests include power system distribution, energy management, power system analysis, renewable energy sources, power markets, and recently power system optimization.

ABDULLAH M. SHAHEEN was born in Tanta, Egypt, in 1985. He received the B.Sc. degree from Suez Canal University, Port-Said, Egypt, in 2007, and the M.Sc. and Ph.D. degrees from Menoufia University, Shebin El-Kom, Egypt, in 2012 and 2016, respectively. He is currently with the Department of Electrical Engineering, Faculty of Engineering, Suez University, El-Suweis, Egypt. His research interests include power system operation, control, planning, the applications of optimization algorithms in electric power systems, renewable integration, and smart grids.

MOHAMED A. TOLBA (Senior Member, IEEE) received the B.Sc. and M.Sc. degrees in electric power and machines engineering from the Faculty of Engineering, Minia University, Minia, Egypt, in 2008 and 2013, respectively, and the Ph.D. degree from the Electric Power Systems Department, Moscow Power Engineering Institute (MPEI), National Research University, Moscow, Russia, in 2019. In 2019, he began an Assistant Professor with the Nuclear Research Center, Reactors Engineering Department, Egyptian Atomic Energy Authority, Cairo, Egypt. He is currently an Assistant Professor (a Visitor) with the Electric Power Systems Department, Moscow Power Engineering Institute, National Research University. His main research interests include power quality management, soft computing applications in electric power networks, renewable distributed energy sources, control systems, and distribution network operation management. Since 2019, he has been serving as the Co-Chair and the Technical Program Chair for the IEEE REEPE Conference.